NASA TN D-1795

TECHNICAL NOTE

D-1795

A COMPARISON OF EXPERIMENTAL AND THEORETICAL RESULTS FOR THE COMPRESSIBLE TURBULENT-BOUNDARY-LAYER SKIN FRICTION WITH ZERO PRESSURE GRADIENT

By John B. Peterson, Jr.

Langley Research Center
Langley Station, Hampton, Va.

NATIONAL AERONAUTICS AND SPACE ADMINISTRATION
WASHINGTON March 1963

NATIONAL AERONAUTICS AND SPACE ADMINISTRATION

TECHNICAL NOTE D-1795

A COMPARISON OF EXPERIMENTAL AND THEORETICAL RESULTS FOR THE COMPRESSIBLE TURBULENT-BOUNDARY-LAYER SKIN FRICTION WITH ZERO PRESSURE GRADIENT

By John B. Peterson, Jr.

SUMMARY

Seven theories of compressible turbulent-boundary-layer skin friction were compared with experimental data in order to determine their accuracy. The seven theories used for comparison were those of Van Driest; Wilson and Van Driest; Cope, Monaghan, and Johnson; and Winkler and Cha; and the T' methods of Sommer and Short, Monaghan, and Eckert. The data were obtained from 21 sources and covered a range of Mach numbers up to 10 and Reynolds number up to 68×10^6 at zero heat transfer and 100×10^6 with heat transfer. The comparison between the theories and experiment was made on one curve by performing a transformation on the experimental data, and the results showed that the Sommer and Short T' method most accurately matched the experimental data. Curves to aid in the calculation of skin friction by the Sommer and Short T' method are presented. Also presented in an appendix are two new methods of finding the virtual origin of the compressible turbulent boundary layer.

INTRODUCTION

An accurate estimation of the turbulent-boundary-layer skin-friction coefficient is very important in the computation of the performance of supersonic vehicles since skin friction comprises a large part of the drag of such vehicles. Also, most methods used to estimate the heat transfer to supersonic vehicles require a knowledge of the skin friction. The state of the art in the prediction of turbulent skin friction at supersonic speeds is not very advanced and there are large differences between various theories. (For example, see the predicted effects of M_δ in fig. 1 of ref. 1.) Also, estimations of the effects of Reynolds number and wall temperature on the turbulent skin-friction coefficient vary widely. (See refs. 2 and 3.)

Since any theory of compressible turbulent skin friction is an approximate solution to the complete differential equation for the turbulent boundary layer and employs many assumptions and empirical constants, the results of the theory must be compared with experiment in order to prove its accuracy. The purpose of

this report is to find the theory which most accurately predicts the effects of Mach number, Reynolds number, and wall temperature ratio on the turbulent skin-friction coefficient in two-dimensional flow. The effects of pressure gradients and real-gas effects were not investigated in this report.

There are many theories of compressible turbulent skin friction (more than 21); however, for the following reasons it was not necessary to use all of them in the correlation. Theories which did not cover the range of the experimental data such as the extended Frankl and Voishel theory (ref. 2), which is restricted to the range $0 \leqq M \geqq 4$, and Tucker's theory (ref. 4), which is for use at zero heat transfer only, could not be used for comparison. Also, many theories have been shown to be at large variance with the experimental data and need not be considered further. (See refs. 1 and 5.) Thus the theories of Van Driest (ref. 6), Wilson and Van Driest (refs. 7 and 8), Cope, Monaghan, and Johnson (refs. 9 and 10), and Winkler and Cha (ref. 11), along with the T' methods of Sommer and Short (ref. 3), Monaghan (ref. 12), and Eckert (ref. 13), were chosen for comparison with the experimental data. These seven theories are probably the most widely used for calculation of the compressible turbulent skin-friction coefficient.

SYMBOLS

A,B,C,J,K,L	constants
C_F	average skin-friction coefficient
C_F^*	transformed average skin-friction coefficient
C_f	local skin-friction coefficient
D	drag
k	mixing-length constant
l	mixing length
M	Mach number
p	pressure, lb/sq in.
R	Reynolds number
R_{le}	Reynolds number based on distance from leading edge
R_{le-x}	Reynolds number based on distance from leading edge to virtual origin of turbulent boundary layer

R_x	Reynolds number based on distance from virtual origin of turbulent boundary layer, $U_\delta x/\nu_\delta$
R_x^*	transformed Reynolds number based on distance from virtual origin of turbulent boundary layer
R_θ	Reynolds number based on momentum thickness of boundary layer, $U_\delta \theta/\nu_\delta$
S	area
s	nondimensional sublayer height, $y_s u_\tau/\nu_w$
T	temperature, $^\circ R$
T'	reference temperature, $^\circ R$
U_δ	velocity outside boundary layer
u	velocity in boundary layer
u_τ	friction velocity, $\sqrt{\frac{\tau_w}{\rho_w}}$
v	friction-velocity ratio, $\frac{U_\delta}{u_\tau} = \sqrt{\frac{2}{C_{f,w}}}$
x	distance from virtual origin of turbulent boundary layer
y	distance from wall
δ	boundary-layer thickness
η_r	recovery factor
θ	momentum thickness of boundary layer
μ	gas viscosity
μ'	gas viscosity evaluated at T'
ν	kinematic viscosity
ρ	gas density
ρ'	gas density evaluated at T' and p_δ
ρ_w	gas density evaluated at T_w and p_δ

τ_w	wall shear stress
ϕ	defined in equation (4)

Subscripts:

aw	adiabatic wall
eff	effective
est	estimated
exp	experimental
i	incompressible
s	sublayer
T'	based on temperature T'
t	total or stagnation condition
th	as given by theory
w	wall or wall conditions
δ	conditions outside the boundary layer

REVIEW OF THEORIES

A very comprehensive review of the theories of turbulent skin friction is given in reference 5. Only the more important points, therefore, will be discussed here.

Incompressible Theory

In incompressible turbulent flow, the use of the mixing-length law of either Prandtl ($l = ky$) or Von Kármán $\left(l = k \frac{du/dy}{d^2u/dy^2}\right)$ leads to the same form for the skin-friction coefficient. By adjusting an arbitrary constant to fit the experimental data, Von Kármán obtained the following equations for incompressible turbulent skin friction:

$$\frac{0.242}{\sqrt{C_F}} = \log_{10}\left(R_x C_F\right) \tag{1}$$

and

$$\frac{C_f}{C_F} = \frac{1}{1 + 3.59\sqrt{C_F}} \tag{2}$$

where

$$C_f = \frac{\tau_w}{\frac{1}{2}\rho_\delta U_\delta^2}$$

$$C_F = \frac{D/S}{\frac{1}{2}\rho_\delta U_\delta^2}$$

A large number of experimental data have been accumulated at subsonic speeds, and the Kármán-Schoenherr equation is generally accepted as the best formula to fit these data. (See ref. 14.) All the compressible turbulent skin-friction theories used in this report reduce to the Kármán-Schoenherr formula for the incompressible conditions of $M_\delta = 0$ and $T_w = T_\delta$.

Compressible Theory

In compressible flow, the two mixing lengths (Von Kármán and Prandtl) do not give the same form for the skin-friction coefficient, as they do in incompressible flow. Therefore, the results obtained by Van Driest (ref. 6) with the Prandtl mixing length are different from those obtained by Wilson (ref. 7) with the Von Kármán mixing length. By using the Prandtl mixing-length hypothesis in compressible flow, Van Driest obtained (in the nomenclature of this report)

$$\frac{0.242}{\sqrt{C_{F,w}}}\phi = \log_{10}\left[C_{F,w}R_{x,w}\left(\frac{T_\delta}{T_w}\right)^{1/2}\right] \tag{3}$$

where

$$C_{F,w} = \frac{D/S}{\frac{1}{2}\rho_w U_\delta^2}$$

$$R_{x,w} = \frac{\rho_w U_\delta x}{\mu_w}$$

$$\phi = \frac{1}{A}\left[\sin^{-1}\frac{A - \frac{B}{2A}}{\sqrt{1 + \left(\frac{B}{2A}\right)^2}} + \sin^{-1}\frac{\frac{B}{2A}}{\sqrt{1 + \left(\frac{B}{2A}\right)^2}}\right] \tag{4}$$

$$A^2 = \frac{T_{aw}}{T_w} - \frac{T_\delta}{T_w} \tag{5}$$

$$B = \frac{T_{aw}}{T_w} - 1 \tag{6}$$

The use of the Von Kármán mixing-length law, however, leads to the following form for the compressible turbulent skin-friction coefficient:

$$\frac{0.242}{\sqrt{C_{F,w}}}\phi = \log_{10}\left(C_{F,w}R_{x,w}\right) \tag{7}$$

which was given by Wilson (ref. 7) for zero heat transfer and Van Driest (ref. 8) for heat transfer.

Among the simplifications used by Van Driest and Wilson was the assumption that the mixing-length hypothesis applied all the way through the boundary layer to the wall. This assumption, which neglects the laminar sublayer, resulted in a simplified formula for ϕ. However, Monaghan (ref. 5) gave another form for ϕ in which the laminar sublayer was included. The ϕ derived by Monaghan (herein designated ϕ_s) was

$$\phi_s = \frac{1}{A}\left[\sin^{-1}\frac{A - \frac{B}{2A}}{\sqrt{1 + \left(\frac{B}{2A}\right)^2}} - \sin^{-1}\frac{A\frac{s}{v} - \frac{B}{2A}}{\sqrt{1 + \left(\frac{B}{2A}\right)^2}} + A\frac{s}{v}\right] \tag{8}$$

where

$$s = \frac{y_s u_\tau}{\nu_w} \tag{9}$$

$$v = \sqrt{\frac{2}{C_{f,w}}} \tag{10}$$

In order to determine whether this form of ϕ gave better results for the compressible turbulent skin friction, both ϕ and ϕ_s were used in the mixing-length theories for comparison with the data. The result of this comparison is discussed subsequently.

The four other theories for turbulent skin friction that are used for comparison in this report (Cope, Monaghan, and Johnson; Winkler and Cha; Sommer and Short T'; Monaghan T'; and Eckert T') are more empirical in nature. Cope (ref. 9) and Monaghan and Johnson (ref. 10) assumed that the equation for the nondimensional velocity profile was the same in compressible flow as in incompressible flow if the wall conditions of density and viscosity were used. Under this assumption the compressible skin-friction formula was found to be

$$\frac{0.242}{\sqrt{C_{F,w}}} = \log_{10}\left(C_{F,w}R_{x,w}\frac{T_\delta}{T_w}\right) \tag{11}$$

Winkler and Cha's method (ref. 11) assumes that the ratio of local skin-friction coefficients $C_f/C_{f,i}$ at constant R_θ can be expressed as a function of T_t/T_δ and T_w/T_{aw} only. In order to fit the data available at that time, Winkler and Cha gave the following equation:

$$\left(C_f/C_{f,i}\right)_{R_\theta=\text{Constant}} = \frac{\left(T_w/T_{aw}\right)^{1/4}}{\left(T_t/T_\delta\right)^{1/2}} \tag{12}$$

Using this equation together with equation (1) results in the following expression for compressible turbulent skin friction:

$$\frac{0.242}{\sqrt{C_F\left(T_t/T_\delta\right)^{1/2}\left(T_w/T_{aw}\right)^{-1/4}}} = \log_{10}\left(C_F R_x\right) \tag{13}$$

The T' method of calculating skin friction is a semiempirical method, based on the formulas for incompressible skin friction, which was developed by Rubesin and Johnson (ref. 15) in 1949 for laminar flow. It was extended for use in compressible turbulent flow by Sommer and Short (ref. 3). In this method, the fluid properties in the flow are evaluated at some intermediate or reference temperature in the boundary layer. This reference temperature is called T' and is a function of the free-stream Mach number and the ratio of wall temperature to free-stream temperature. These properties are then used in the incompressible turbulent skin-friction formula to obtain the skin friction. Thus

$$\frac{0.242}{\sqrt{C_{F,T'}}} = \log_{10}\left(R_{x,T'}C_{F,T'}\right) \tag{14}$$

where

$$R_{x,T'} = \frac{\rho' U_\delta x}{\mu'} \tag{15}$$

$$C_{F,T'} = \frac{D/S}{\frac{1}{2}\rho' U_\delta^2} \tag{16}$$

Sommer and Short found that the following equation for the reference temperature T' matched their experimental data and the data of Coles (ref. 16) and Chapman and Kester (ref. 1):

$$\frac{T'}{T_\delta} = 1 + 0.035 M_\delta^2 + 0.45\left(\frac{T_w}{T_\delta} - 1\right) \tag{17}$$

Monaghan (ref. 12) proposed the following equation for T':

$$\frac{T'}{T_\delta} = 1 + 0.0284 M_\delta^2 + 0.54\left(\frac{T_w}{T_\delta} - 1\right) \tag{18}$$

In 1954 Eckert (ref. 13) proposed the following equation for T':

$$\frac{T'}{T_\delta} = 1 + 0.044 \eta_r M_\delta^2 + 0.5\left(\frac{T_w}{T_\delta} - 1\right) \tag{19}$$

Using a recovery factor η_r of 0.89 results in

$$\frac{T'}{T_\delta} = 1 + 0.0392 M_\delta^2 + 0.5\left(\frac{T_w}{T_\delta} - 1\right) \tag{20}$$

EXPERIMENTAL DATA

The results of many different experimental investigations of supersonic turbulent skin friction (refs. 1, 2, 3, 7, 10, and 16 to 29) were compared with the theories. These experiments cover Mach numbers from 1.5 to 10 and Reynolds numbers from 1 to 68 $\times 10^6$ at zero heat transfer, and Mach numbers from 1.7 to 10 and Reynolds numbers from 2 to 100 $\times 10^6$ at ratios of wall to equilibrium temperature from 0.17 to 1.8. The experimental conditions at which the skin-friction values were obtained are shown for each reference in tables I and II. Not all experiments on compressible turbulent skin friction are suitable for comparison with the theories; only data which represented as nearly as possible the skin friction in two-dimensional flow with zero pressure gradient and without dissociation or ionization were used. Also, only experiments in which the effective Reynolds number could be determined were used.

In order to give equal weight to each experiment, only one or two points were plotted at each Mach number in the comparisons with theories. Usually one representative point at the lower and one at the higher Reynolds number was used, if a large enough range of Reynolds number was covered in the experiment, in order to give an indication of the trend of the data with Reynolds number.

Measurement of Skin Friction

Many different procedures have been used to determine the skin-friction coefficient in flat-plate flow. The procedure used in each reference of tables I and II is shown in column 19. A brief description of each method is given below.

Drag.- The total skin-friction drag of a body such as a hollow cylinder or cone-cylinder is obtained by subtracting the forebody and base drags from the measured drag. Usually some means must be used to measure the boundary-layer profiles at the beginning of the test area of the model in order to determine the virtual origin of the turbulent boundary layer. The determination of the virtual origin, and therefore of the Reynolds number associated with the measured skin-friction coefficient, is very important to the accuracy of the experiment and is discussed in a subsequent section.

Momentum.- By measuring the momentum loss in the boundary layer, the drag of the surface on which the momentum loss occurred can be computed. The momentum loss can be determined by measuring the boundary-layer velocity profile and computing the momentum thickness from the formula

$$\theta = \int_0^{\delta} \frac{\rho u}{\rho_\delta U_\delta}\left(1 - \frac{u}{U_\delta}\right)dy \tag{21}$$

where $\rho_\delta U_\delta{}^2\theta$ is the rate of loss of momentum in the boundary layer per unit width of the flat plate. The average skin-friction coefficient is then

$$C_F = 2\frac{\theta}{x} = 2\frac{R_\theta}{R_x} \tag{22}$$

Here, the importance of accurately determining the virtual origin of the turbulent boundary layer is obvious, since the average skin-friction coefficient is inversely proportional to the distance from the virtual origin to the place of measurement. Thus any error in determining the effective Reynolds number will cause an error in the average skin-friction coefficient.

Skin-friction balance.- By mounting a small section of the surface on a sensitive balance, the local surface shear can be determined. However, as before, supplementary measurements of the boundary layer must be made to determine the effective Reynolds number.

Velocity slope at the wall.- Measurements of velocity profiles in a turbulent boundary layer have shown that a thin laminar sublayer exists near the wall. In this sublayer the velocity increases linearly with distance from the surface. Therefore, by using a very small probe in a thick boundary layer, the slope of the velocity profile at the wall can be determined. The wall shear stress can then be determined from the viscosity and the velocity gradient at the wall. Fortunately, the sublayer thickness increases with increasing Mach number and, therefore, this method becomes more practical at high Mach numbers.

Determination of the Virtual Origin of the Turbulent Boundary Layer

In theoretical analyses of turbulent boundary layers a basic parameter is the Reynolds number based on the length of turbulent flow, where it is assumed that a fully developed turbulent boundary layer originates at the leading edge. Experimentally, however, some laminar flow exists near the leading edge, followed by a transition region and then by fully developed turbulent flow (see fig. 1). Therefore, in analyses of experimental results, the conditions and rate of growth of the turbulent boundary layer at a given position are assumed to be equivalent to the conditions in a fully turbulent boundary layer originating at a position behind the leading edge. This fictitious origin of the turbulent boundary layer is referred to as the virtual origin (fig. 1) and the Reynolds number based on the length from the virtual origin is the effective Reynolds number of the turbulent boundary layer.

Various methods are used to find the position of the virtual origin. The method most commonly used is extrapolation of the boundary-layer momentum thickness, measured in the turbulent portions of the boundary layer, to zero. The virtual origin of the turbulent boundary layer is then taken to be the point where the momentum thickness would have been zero if the boundary layer had always been turbulent. The extrapolation of the momentum thickness θ can be accomplished by any one of many different procedures. In the present report three different methods of extrapolating θ to zero were applied to the experimental data where possible, and the results are shown in columns 11, 12, and 13 of tables I and II.

The method shown in column 11 is described in appendix A. This method is essentially an extrapolation of the measured values of R_θ and R_{le} by a power law of the form

$$R_\theta = K\left(R_{le} - R_{le-x}\right)^C \tag{23}$$

The method of least squares is used to adjust the three arbitrary constants K, R_{le-x}, and C to fit the data.

A second method, shown in column 12 of tables I and II, was proposed by Rubesin, Maydew, and Varga (ref. 2). In this method the data are fitted to a curve of the form

$$R_\theta = K\left(R_{le} - R_{le-x}\right)^C = KR_x{}^C \tag{24}$$

where C is a known constant. The data are plotted on log-log paper and the value of R_x necessary to match the slope of the line to the constant C is determined. The constant C is obtained by averaging the values predicted by several theories; its value is approximately the same for the various theories and it is relatively insensitive to changes in Reynolds number. Calculation of C can be made simply by noting that

$$C = \frac{d\left(\log R_\theta\right)}{d\left(\log R_x\right)} = \frac{dR_\theta}{dR_x}\frac{R_x}{R_\theta} = \frac{C_f}{C_F} \tag{25}$$

since

$$C_f = 2\frac{dR_\theta}{dR_x} \tag{26}$$

$$C_F = 2\frac{R_\theta}{R_x} \tag{27}$$

The value of C_f/C_F is easily found from figure 2 with the use of a transformed Reynolds number $R_x{}^*$ (presented in table III for various theories) as discussed in appendix B. A more complete discussion of the transformed Reynolds number $R_x{}^*$ is presented in the section entitled "Results and Discussion."

The results of a third method of extrapolating θ to zero are shown in column 13 of tables I and II. This method utilizes measured values of local skin-friction coefficient and boundary-layer momentum thickness to extrapolate the momentum thickness to zero; the extrapolation of the momentum thickness is accomplished by assuming that an affine transformation exists between the incompressible and the compressible values of R_θ and C_f and that the transformation is

a function only of the Mach number and wall temperature ratio T_w/T_δ. The details of the procedure for finding the transformation are given in appendix A. After the transformation is found, the value of R_x for the measured compressible C_f can be found.

Results of another method for finding the virtual origin are shown in column 14 of tables I and II. In this method it is assumed that the boundary-layer growth and shear distributions are similar to the sketches of figure 1. The virtual origin is then assumed to be at approximately the same location as the point of minimum shear. This point is at the end of the laminar boundary layer and the beginning of natural transition on a flat plate. Although this method does not have the theoretical basis of the methods of extrapolating momentum thickness, it is more convenient experimentally and the virtual origin can be quickly and easily found.

The effective Reynolds number for each reference was determined by every method for which sufficient information was available. All the data in each experiment were used to find the effective Reynolds number, even though only one or two points are shown in the tables and plotted in the comparisons with the theories. The reference author's estimate of the effective Reynolds number of his own experiment is given in column 15. Average effective Reynolds numbers, obtained from columns 11 to 15, are presented in column 16 of tables I and II to be used for application to the experimental data. The effective Reynolds number for reference 3 in table II is discussed in appendix C.

RESULTS AND DISCUSSION

The experimental data shown in tables I and II were measured through a large range of M_δ, R_x, T_w, and T_δ. Inasmuch as the theoretical skin friction is a function of all these flow parameters, a comparison of these experimental data with the theories could be accomplished through the use of a series of curves prepared for the given test conditions. Such an arrangement, however, would result in a complicated comparison. By means of the following procedure the comparison of the data with the theories can be accomplished through the use of one curve.

Examination of the compressible turbulent skin-friction theories (eqs. (3), (7), (11), (13), and (14)) shows a close similarity to the Kármán-Schoenherr equation for incompressible skin friction (eq. (1)). In fact, if the compressible skin-friction formulas are rearranged they can be put into the same form as the Kármán-Schoenherr equations except that the skin-friction coefficient and Reynolds number are modified by certain functions of the Mach number, wall temperature, and free-stream temperature to account for the effect of compressibility. If the modified or transformed skin-friction coefficient and Reynolds number are denoted by asterisks, each of the theoretical equations for compressible skin friction can be written as

$$\frac{0.242}{\sqrt{C_F^*}} = \log_{10}\left(R_x^* C_F^*\right) \tag{28}$$

The form of the modified Reynolds number R_x^* and skin-friction coefficient C_F^* for each theory is shown in table III. These modifications are seen to be a function of M_δ, T_w, and T_δ only. The theoretical variation of the modified or transformed skin-friction coefficient C_F^* with Reynolds number R_x^* can be represented by a single line for all conditions of M_δ, T_w, and T_δ. This line is the same as the Kármán-Schoenherr curve of incompressible skin-friction coefficient. Experimental results can then be reduced in accordance with each of the theories and compared with the theoretical line. The experimental R_x and C_F values shown in tables I and II are reduced in accordance with table III to obtain the transformed Reynolds number R_x^* and skin-friction coefficient C_F^*.

In order to eliminate a separate plot for local skin friction, the local-skin-friction coefficients were converted to average-skin-friction coefficients by dividing them by the value of $\left(C_f/C_F\right)_{th}$, where $\left(C_f/C_F\right)_{th}$ was obtained from the particular theory involved. These points were then plotted on the average-skin-friction plots. The comparison of a local-skin-friction value divided by $\left(C_f/C_F\right)_{th}$ with the average-skin-friction curve is the same as a comparison of the local-skin-friction value with a local-skin-friction curve except for a change in the magnitude of the ordinate by the factor $\left(C_f/C_F\right)_{th}$. However, a logarithmic scale on the ordinate presents the same comparison between theory and experiment by either method, since

$$\log C_{f,exp} - \log C_{f,th} = \log \frac{C_{f,exp}}{\left(C_f/C_F\right)_{th}} - \log \frac{C_{f,th}}{\left(C_f/C_F\right)_{th}}$$

$$= \log \frac{C_{f,exp}}{\left(C_f/C_F\right)_{th}} - \log C_{F,th} \qquad (29)$$

The transformed Reynolds number R_x^* and transformed skin-friction coefficient C_F^* obtained from data taken at zero heat transfer are plotted in figures 3 to 11. The references corresponding to the data symbols for these figures are shown in table I. Data taken with heat transfer are shown in table II and are plotted in figures 12 to 20. The references corresponding to the data symbols for these figures are shown in table II.

A comparison between the two mixing-length theories shows that the Von Kármán mixing length gives better results at zero heat transfer than the Prandtl mixing length. This can be seen by comparing Wilson's and Van Driest's theories (refs. 7 and 8) in figure 3, where the Von Kármán mixing length is used, with Van Driest's theory (ref. 6) in figure 5, where the Prandtl mixing length is used. Since the Von Kármán mixing length gives better results than the Prandtl mixing length with zero heat transfer, it might be expected to give better results with heat transfer

also. However, under conditions of heat transfer there is little difference between the correlations obtained with the Von Kármán mixing length (fig. 12) and the Prandtl mixing length (fig. 14). This result is believed to be at least partly due to experimental scatter in the data taken with heat transfer. More scatter is to be expected in these data because of the difficulty in obtaining skin-friction results with heat transfer.

Originally it was believed that taking the laminar sublayer into account as suggested by Monaghan (ref. 5) would improve the accuracy of Van Driest's (Prandtl mixing length) and Wilson's and Van Driest's (Von Kármán mixing length) theories. This improvement can be noted by comparing figures 3 and 5 with figures 4 and 6, where a nondimensional sublayer height s of 11.6 was used. However, a comparison of figures 12 and 14 with figures 13 and 15 shows that taking the sublayer into account decreased the agreement between theory and experiment under conditions of heat transfer in almost every case. Although the nondimensional sublayer height s will depend on the wall heat-transfer rate, the variation is believed to be small. In any case a sublayer exists, but apparently neglecting it altogether gives better agreement with experimental data under conditions of heat transfer.

A careful examination of all the figures shows that the semiempirical T' methods of Sommer and Short, Monaghan, and Eckert generally give the best agreement with the experimental data, especially at zero heat transfer, the Sommer and Short T' method being slightly better than the Monaghan and Eckert T' methods (see figs. 9, 10, and 11). Therefore, since the Sommer and Short T' method gives the best correlation with zero-heat-transfer data and one of the better correlations with data taken with heat transfer, it appears that the Sommer and Short method will provide the most accurate estimate of the compressible turbulent skin-friction drag within the range of Mach number, Reynolds number, and wall heat transfer of the experimental data.

CONCLUDING REMARKS

The large scatter in the available experimental data prevents an exact determination of the compressible turbulent skin friction, especially with heat transfer. More data at Mach numbers greater than 6 are needed, since there is a larger difference among the theories at high Mach numbers. Only one experiment at zero heat transfer and two experiments with heat transfer were available for comparison with the theories above $M = 6$.

Of the seven theories compared with the experimental data, the empirical T' methods agreed most closely with the data. The Sommer and Short T' method appears to provide the most accurate estimate of the compressible turbulent skin friction within the range of Mach number, Reynolds number, and wall heat transfer of the available experiments. However, to apply this method with confidence beyond the present experimental limits will require further experimental verification.

A comparison of the mixing-length theories of Wilson and Van Driest based on the Von Kármán mixing length with that of Van Driest based on the Prandtl mixing

length indicates that the Von Kármán mixing length gives better agreement with experiment. Taking the laminar sublayer into account improved the agreement between theory and experiment at zero heat transfer but reduced the agreement under conditions of heat transfer.

Langley Research Center,
National Aeronautics and Space Administration,
Langley Station, Hampton, Va., February 26, 1963.

APPENDIX A

METHODS OF DETERMINING THE VIRTUAL ORIGIN OF A TURBULENT BOUNDARY LAYER BY EXTRAPOLATING θ TO ZERO

Method of Least Squares

As stated in the body of the report, a commonly used method of determining the virtual origin is to measure the momentum thickness at several stations in the turbulent portions of the boundary layer. These momentum thicknesses are then extrapolated to zero in order to determine the virtual origin. One way of extrapolating θ to zero is to use the method of least squares to fit a mathematical curve of the following form to the measured data:

$$R_\theta = K\left(R_{le} - R_{le-x}\right)^C$$

where

K,C arbitrary constants to be determined by the method of least squares

R_θ Reynolds number based on momentum thickness

R_{le} Reynolds number based on distance from leading edge

R_{le-x} Reynolds number based on distance from leading edge to virtual origin, to be determined by the method of least squares

In order to apply the method of least squares, it is convenient to transform the equation to

$$\log R_\theta = \log K + C \log\left(R_{le} - R_{le-x}\right)$$

and linearize this equation by a Taylor's series for the last term, so that

$$\log R_\theta = \log K + C_{est} \log\left[R_{le} - \left(R_{le-x}\right)_{est}\right] + \log\left[R_{le} - \left(R_{le-x}\right)_{est}\right]\Delta C$$

$$- \frac{0.434 C_{est}}{R_{le} - \left(R_{le-x}\right)_{est}} \Delta R_{le-x}$$

where

$C_{est}, \left(R_{le-x}\right)_{est}$ estimated values of C and R_{le-x}

ΔC difference between the true value of C and the estimated value C_{est}

ΔR_{le-x} difference between the true value of R_{le-x} and the estimated value $\left(R_{le-x}\right)_{est}$

The three quantities $\log K$, ΔC, and ΔR_{le-x} can then be solved for by the method of least squares with appropriate assumptions for C_{est} and $\left(R_{le-x}\right)_{est}$. The three unknown constants are then

$$K = \log^{-1}(\log K)$$

$$R_{le-x} = \left(R_{le-x}\right)_{est} + \Delta R_{le-x}$$

$$C = C_{est} + \Delta C$$

The value of R_{le} at which R_θ is zero (i.e., the Reynolds number of the virtual origin), is obviously then equal to R_{le-x} and the effective Reynolds number is

$$R_x = R_{le} - R_{le-x}$$

The values of the effective Reynolds number that were obtained for the experimental data used in the report by the least-squares method are shown in column 11 of tables I and II.

Virtual Origin From Measurements of C_f and R_θ

In many investigations of compressible turbulent skin friction, only the Reynolds number based on the boundary-layer momentum thickness R_θ and the local skin-friction coefficient C_f are measured. However, for this report it is necessary to know the value of R_x for the measured local-skin-friction coefficient. If C_f is known for every value of R_θ, then the R_x corresponding to each R_θ and, therefore, each C_f can be found. This can be shown by noting that

$$C_f = 2 \frac{dR_\theta}{dR_x}$$

Then

$$R_x = \int_0^{R_x} dR_x = \int_0^{R_\theta} \frac{2}{C_f} dR_\theta \tag{A1}$$

Usually, however, the values of C_f are measured over only a small range of R_θ in an experiment. The problem, therefore, is to make a suitable estimate of the C_f values at lower values of R_θ. One method, which was used by Korkegi, is to assume that the ratio $C_f/C_{f,i}$ is a constant and independent of R_θ; thus R_x can be determined by integration or by use of a plot of C_f against R_θ. (See ref. 24.)

Measurements of $C_f/C_{f,i}$, however, have shown that this ratio varies slightly, and most theories predict some variation in $C_f/C_{f,i}$ with R_θ. Therefore, the following procedure, which allows for some variation in $C_f/C_{f,i}$, is believed to give more valid results.

As stated previously, the problem is to find a suitable assumption for the variation of C_f with R_θ below the range of the experiment. In this procedure it is assumed that there is an affine transformation between the incompressible curve and the compressible curve of $C_{f,i}$ against $R_{\theta,i}$. That is,

$$\left.\begin{aligned} C_f &= JC_{f,i} \\ R_\theta &= LR_{\theta,i} \end{aligned}\right\} \tag{A2}$$

Each of the seven theories used in this report supports this assumption, inasmuch as they all predict that such a transformation exists. This fact can be shown by noting that

$$\left.\begin{aligned} C_F &= \frac{C_F}{C_F^*} C_{F,i} \\ R_x &= \frac{R_x}{R_x^*} R_{x,i} \end{aligned}\right\} \tag{A3}$$

where C_F^* and R_x^* are the modified skin-friction coefficient and Reynolds number discussed in the section "Results and Discussion." Therefore, since

$$\left.\begin{aligned} C_f &= C_F + R_x \frac{dC_F}{dR_x} \\ R_\theta &= \frac{1}{2} R_x C_F \end{aligned}\right\} \tag{A4}$$

substituting equations (A3) into (A4) yields

$$C_f = \frac{C_F}{C_F^*} C_{f,i}$$

$$R_\theta = \frac{C_F}{C_F^*} \frac{R_x}{R_x^*} R_{\theta,i}$$

The parameters C_F/C_F^* and R_x/R_x^* are dependent only on the values of M_δ, T_w, and T_δ, as can be determined from table III. Thus, under constant conditions of M_δ, T_w, and T_δ, these parameters are constant and the theories predict an affine transformation of the incompressible skin-friction curve to the compressible skin-friction curve.

The constant parameters of the transformation are not known beforehand and must be found from the experimental data. This is accomplished in the following manner. The data are plotted in the form of $\log C_f$ against $\log R_\theta$, along with the incompressible Kármán-Schoenherr curve, as shown in the following sketch:

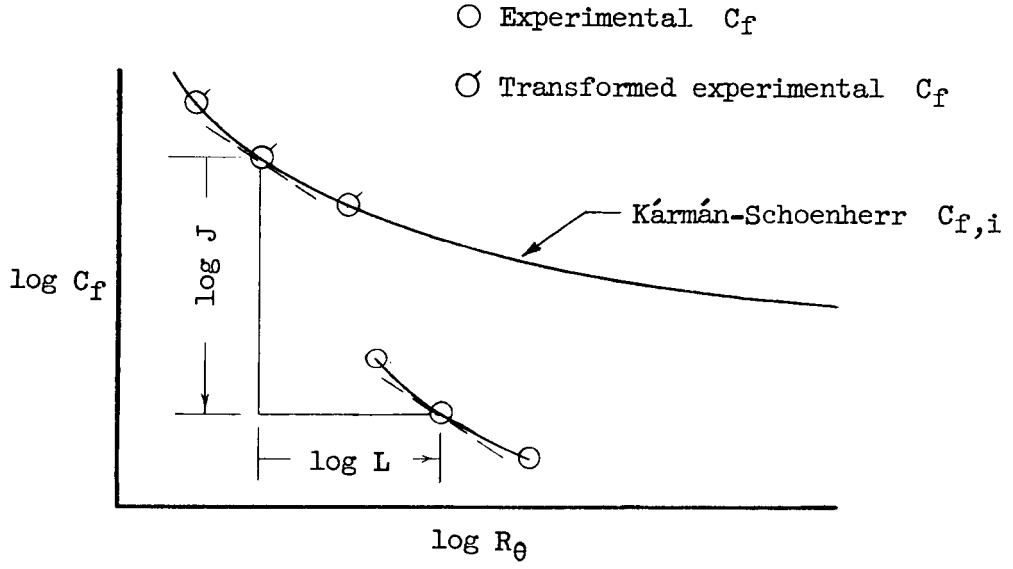

The constants J and L can then be found by matching the slope of the experimental curve of $\log C_f$ against $\log R_\theta$ with that of the incompressible curve. The values of R_x for the measured values of C_f can then be found from

$$R_x = \frac{L}{J}\left(R_{x,i}\right)_{C_{f,i}=\text{Transformed } C_f}$$

which is obtained by substitution of equations (A2) into equation (A1). Thus the value of R_x for the measured value of C_f is simply the incompressible Reynolds

number, corresponding to the incompressible local skin-friction coefficient, multiplied by L/J.

This method of finding R_x is relatively insensitive to errors in finding the transformation constants J and L. For example, a 50-percent change in the value of L for reference 19 was found to change the value of R_x from 19.3×10^6 to 19.5×10^6 at $M = 1.73$, or only 1 percent. Also, the values of R_x obtained by this method are seen in table I to compare favorably with those obtained by the three other methods used for reference 19.

The R_x found by this method will possess an internal consistency which is necessary for any method of determining R_x from C_f and R_θ. For consistency, it is required that

$$R_{x,2} - R_{x,1} = \int_{R_{\theta,1}}^{R_{\theta,2}} \frac{2}{C_f} \, dR_\theta$$

where the subscripts 1 and 2 refer to longitudinal stations along the flat plate. This equation is automatically satisfied by this method of finding R_x, since

$$\int_{R_{\theta,1}}^{R_{\theta,2}} \frac{2}{C_f} \, dR_\theta = \int_{R_{\theta,i,1}}^{R_{\theta,i,2}} \frac{2}{JC_{f,i}} \, L \, dR_{\theta,i} = \frac{L}{J}\left(R_{x,i,2} - R_{x,i,1}\right) = R_{x,2} - R_{x,1}$$

where the third step is obtained from the internal consistency of the incompressible relations. Thus it is believed that this method will give accurate estimates of R_x for experiments in which only C_f and R_θ are given.

APPENDIX B

CALCULATION OF TURBULENT C_F, C_f, AND C_f/C_F BY THE SOMMER AND SHORT T' METHOD

Figures 2 and 21 to 24 were prepared to help simplify the procedure for finding the average turbulent skin-friction coefficient C_F, the local turbulent skin-friction coefficient C_f, and their ratio C_f/C_F by the Sommer and Short T' method. With a given Mach number M_δ, wall temperature ratio T_w/T_δ, and Reynolds number $R_{x,\delta}$, the following procedure should be used:

1. Determine T'/T_δ from figure 21

2. Determine $R_{x,T'}/R_{x,\delta}$ from figure 22

3. Calculate $R_{x,T'}$ from

$$R_{x,T'} = R_{x,\delta} \frac{R_{x,T'}}{R_{x,\delta}}$$

4. Determine either $C_{f,T'}$ or $C_{F,T'}$ from figure 23 or 24

5. Calculate C_f or C_F from the equation

$$C_f = \frac{C_{f,T'}}{T'/T_\delta}$$

or

$$C_F = \frac{C_{F,T'}}{T'/T_\delta}$$

The ratio C_f/C_F is useful in calculation of the virtual origin by the method proposed by Rubesin, Maydew, and Varga (ref. 2). In this method the slope of $\log R_\theta$ against $\log R_x$ must be found. This slope is equal to C_f/C_F since

$$\frac{C_f}{C_F} = \frac{2\frac{dR_\theta}{dR_x}}{2\frac{R_\theta}{R_x}} = \frac{d \log R_\theta}{d \log R_x}$$

The ratio C_f/C_F can be determined from figure 2 after $R_{x,T'}$ is determined from step 3 above. It should also be noted that C_f/C_F can easily be found by any other theory by determining the transformed Reynolds number R_x^* for that theory as shown in table III.

APPENDIX C

DETERMINATION OF EFFECTIVE REYNOLDS NUMBER FOR THE SOMMER AND SHORT DATA

Sommer and Short (ref. 3) tested hollow cylindrical models which were fired down a ballistic range at Mach numbers of 2.8 and 3.8, and also against the airstream in a supersonic tunnel in order to obtain Mach numbers as high as 7.0. The drag was measured on two models which were identical except for a difference in length. The drag of the shorter model ("tare" model) was then subtracted from the drag of the larger one ("test" model). The difference between the drags of the two models then represented the skin friction over the rear portion of the test model. The skin friction measured in this way is neither an average skin friction, since it is not measured from the beginning of the boundary layer, nor a local skin friction, since it was not measured at a local station. For use in this report, it was decided to treat the measured skin friction as a local skin friction since the effective Reynolds number at the end of the tare model was a large percentage of the effective Reynolds number at the end of the test model (20 percent to 40 percent). The problem, then, was to determine what intermediate Reynolds number, between the beginning and the end of the surface on which the skin friction was measured, should be considered as the effective Reynolds number $R_{x,eff}$. It is apparent that $R_{x,eff}$ should be chosen so that the local skin-friction coefficient $\left(C_f\right)_{R_{x,eff}}$ at that point is the same as the measured skin-friction coefficient over the entire measuring surface $C_{f,bc}$. Then

$$C_{f,bc} = \left(C_f\right)_{R_{x,eff}}$$

where

b distance of the beginning of the test surface from the virtual origin of the turbulent boundary layer

c distance of the end of the test surface from the virtual origin of the turbulent boundary layer

$C_{f,bc}$ measured skin-friction coefficient on the test surface from b to c

$\left(C_f\right)_{R_{x,eff}}$ local skin-friction coefficient at $R_{x,eff}$

$R_{x,eff}$ effective Reynolds number for the measured skin-friction coefficient when considered as a local skin-friction coefficient

In order to determine $R_{x,eff}$ it is necessary to assume some relationship for the local skin-friction coefficient. The power law is a good representation of C_f for small ranges of R_x:

$$C_f = AR_x^B$$

Then, since

$$C_{f,bc} = \frac{1}{R_c - R_b} \int_{R_b}^{R_c} C_f \, dR_x = \left(C_f\right)_{R_{x,eff}} = A\left(R_{x,eff}\right)^B$$

solving for the effective Reynolds number gives

$$R_{x,eff} = \left[\frac{R_c^{B+1} - R_b^{B+1}}{(B + 1)\left(R_c - R_b\right)}\right]^{1/B}$$

The average value of B for all the theories was used in calculation of $R_{x,eff}$. The value of B for any of the theories was always within 0.5 percent of the average for all the theories. The value of $R_{x,eff}$ as determined in this way was then entered in column 16 of table II and used for the effective Reynolds number of Sommer and Short's experimental data.

REFERENCES

1. Chapman, Dean R., and Kester, Robert H.: Turbulent Boundary-Layer and Skin-Friction Measurements in Axial Flow Along Cylinders at Mach Numbers Between 0.5 and 3.6. NACA TN 3097, 1954.

2. Rubesin, Morris W., Maydew, Randall C., and Varga, Steven A.: An Analytical and Experimental Investigation of the Skin Friction of the Turbulent Boundary Layer on a Flat Plate at Supersonic Speeds. NACA TN 2305, 1951.

3. Sommer, Simon C., and Short, Barbara J.: Free-Flight Measurements of Turbulent-Boundary-Layer Skin Friction in the Presence of Severe Aerodynamic Heating at Mach Numbers From 2.8 to 7.0. NACA TN 3391, 1955.

4. Tucker, Maurice: Approximate Calculation of Turbulent Boundary-Layer Development in Compressible Flow. NACA TN 2337, 1951.

5. Monaghan, R. J.: A Review and Assessment of Various Formulae for Turbulent Skin Friction in Compressible Flow. Tech. Note No. Aero. 2182, British R.A.E., Aug. 1952.

6. Van Driest, E. R.: Turbulent Boundary Layer in Compressible Fluids. Jour. Aero. Sci., vol. 18, no. 3, Mar. 1951, pp. 145-160, 216.

7. Wilson, Robert E.: Turbulent Boundary-Layer Characteristics at Supersonic Speeds - Theory and Experiment. Jour. Aero. Sci., vol. 17, no. 9, Sept. 1950, pp. 585-594.

8. Van Driest, E. R.: The Turbulent Boundary Layer With Variable Prandtl Number. Rep. No. AL-1914, North American Aviation, Inc., Apr. 2, 1954.

9. Cope, W. F.: The Turbulent Boundary Layer in Compressible Flow. R. & M. No. 2840, British A.R.C., Nov. 1943.

10. Monaghan, R. J., and Johnson, J. E.: The Measurement of Heat Transfer and Skin Friction at Supersonic Speeds. Part II - Boundary Layer Measurements on a Flat Plate at $M = 2.5$ and Zero Heat Transfer. C.P. No. 64, British A.R.C., Dec. 1949.

11. Winkler, Eva M., and Cha, Moon H.: Investigation of Flat Plate Hypersonic Turbulent Boundary Layers With Heat Transfer at a Mach Number of 5.2. NAVORD Rep. 6631 (Aerod. Res. Rep. No. 60), U.S. Naval Ord. Lab. (White Oak, Md.), Sept. 15, 1959.

12. Monaghan, R. J.: On the Behavior of Boundary Layers at Supersonic Speeds. Fifth International Aeronautical Conference. (Los Angeles, Calif., June 20-23, 1955), Inst. Aero. Sci., Inc., 1955, pp. 277-315.

13. Eckert, Ernst R. G.: Survey on Heat Transfer at High Speeds. WADC Tech. Rep. 54-70, U.S. Air Force, Apr. 1954.

14. Locke, F. W. S., Jr.: Recommended Definition of Turbulent Friction in Incompressible Fluids. NAVAER DR Rep. No 1415, Bur. Aero., June 1952.

15. Rubesin, M. W., and Johnson, H. A.: A Critical Review of Skin-Friction and Heat-Transfer Solutions of the Laminar Boundary Layer of a Flat Plate. Trans. A.S.M.E., vol. 71, no. 4, May 1949, pp. 383-388.

16. Coles, Donald: Measurements in the Boundary Layer on a Smooth Flat Plate in Supersonic Flow. III. Measurements in a Flat-Plate Boundary Layer at the Jet Propulsion Laboratory. Rep. No. 20-71 (Contract No. DA-04-495-Ord 18), Jet Propulsion Lab., C.I.T., June 1, 1953.

17. Hakkinen, Raimo J.: Measurements of Turbulent Skin Friction on a Flat Plate at Transonic Speeds. NACA TN 3486, 1955.

18. O'Donnell, Robert M.: Experimental Investigation at a Mach Number of 2.41 of Average Skin-Friction Coefficients and Velocity Profiles for Laminar and Turbulent Boundary Layers and an Assessment of Probe Effects. NACA TN 3122, 1954.

19. Shutts, W. H., Hartwig, W. H., and Weiler, J. E.: Final Report on Turbulent Boundary-Layer and Skin-Friction Measurements on a Smooth, Thermally Insulated Flat Plate at Supersonic Speeds. DRL-364, CM-823 (Contract NOrd-9195), Univ. of Texas, Jan. 5, 1955.

20. Wade, John H. T.: An Experimental Investigation of the Effect of Surface Roughness on the Drag of a Cone-Cylinder Model at a Mach Number of 2.48. Rep. No. 34, Inst. Aerophys., Univ. of Toronto, Sept. 1955.

21. Monaghan, R. J., and Cooke, J. R.: The Measurement of Heat Transfer and Skin Friction at Supersonic Speeds. Part IV - Tests on a Flat Plate at $M = 2.82$. C.P. No. 140, British A.R.C., June 1952.

22. Brinich, Paul F., and Diaconis, Nick S.: Boundary-Layer Development and Skin Friction at Mach Number 3.05. NACA TN 2742, 1952.

23. Goddard, Frank E., Jr.: Effect of Uniformly Distributed Roughness on Turbulent Skin-Friction Drag at Supersonic Speeds. Rep. No. 20-113 (Contract No. DA-04-495-Ord 18), Jet Propulsion Lab., C.I.T., Sept. 3, 1957.

24. Korkegi, Robert H.: Transition Studies and Skin-Friction Measurements on an Insulated Flat Plate at a Mach Number of 5.8. Jour. Aero. Sci., vol. 23, no. 2, Feb. 1956, pp. 97-107, 192.

25. Matting, Fred W., Chapman, Dean R., Nyholm, Jack R., and Thomas, Andrew G.: Turbulent Skin Friction at High Mach Numbers and Reynolds Numbers in Air and Helium. NASA TR R-82, 1961.

26. Pappas, C. C.: Measurement of Heat Transfer in the Turbulent Boundary-Layer on a Flat Plate in Supersonic Flow and Comparison With Skin Friction Results. NACA TN 3222, 1954.

27. Monaghan, R. J., and Cooke, J. R.: The Measurement of Heat Transfer and Skin Friction at Supersonic Speeds. Part III - Measurements of Overall Heat Transfer and of the Associated Boundary Layers on a Flat Plate at $M_1 = 2.43$. C.P. No. 139, British A.R.C., Dec. 1951.

28. Swanson, Andrew G., Buglia, James J., and Chauvin, Leo T.: Flight Measurements of Boundary-Layer Temperature Profiles on a Body of Revolution (NACA RM-10) at Mach Numbers From 1.2 to 3.5. NACA TN 4061, 1957.

29. Hill, F. K.: Appendix II - Skin Friction and Heat Transfer Measurements at Mach Numbers From 8-10 in Turbulent Boundary Layers. TG-14-37, vol. I, Appl. Phys. Lab., Johns Hopkins Univ., May 1959, pp. 15-26.

TABLE I

SUMMARY OF EXPERIMENTAL DATA TAKEN AT ZERO HEAT TRANSFER

1	2	3	4	5	6	7	8	9	10	11	12	13	14	15	16	17	18	19
Symbol	Ref.	Author	M_δ	p_t, psia	T_t, °R	T_δ, °R	$\frac{T_w}{T_\delta}$	R_θ	R_{le-x}	R_x found from -					Average R_x	C_f	C_F	Method of measurement (a)
										Extrapolated θ	Ref. 2	$C_f(R_\theta)$	Min. shear	Author's estimate				
▽	17	Hakkinen	1.48	15.2	600	417	1.41	2.34×10^3	1.29×10^6			1.22		1.04	1.13×10^6	3.02×10^{-3}		SFB
▱	18	O'Donnell	2.41	44.2	565	261	2.08	3.03×10^3	4.11×10^6	1.9	2.4			2.11	2.14×10^6		2.83×10^{-3}	θ
			2.41	58.9	580	268	2.08	6.60	7.60	6.8	5.9			5.70	6.13		2.15	
◇	10	Monaghan and Johnson	2.43	13.7	551	252	2.06	3.95×10^3	3.17×10^6	2.9	2.9		2.6	2.90	2.83×10^6		2.79×10^{-3}	θ
◇	2	Rubesin, Maydew, and Varga	2.45	30.0	560	254	2.06	4.62×10^3	2.98×10^6	2.6	3.7			3.70	3.33×10^6		2.78×10^{-3}	θ
			2.45	40.0	560	254	2.06	7.16	5.30	4.7	6.2			6.20	5.70		2.51	
◺	19	Shutts, Hartwig, and Weiler	1.73	27.5	610	382	1.53	[b]7.7x10³	5.50×10^6	6.2	5.8	6.1		6.5	6.15×10^6	2.10×10^{-3}		SFB
▽			1.73	27.5	610	382	1.53	[b]20.8	19.0	19.7	19.3	19.3		19.3	19.40	1.73		
◺			2.00	34.2	610	339	1.70	[b]7.5	6.13	6.8	6.1	6.6		7.0	6.63	1.94		
◺			2.00	34.2	610	339	1.70	[b]19.0	18.67	19.4	18.7	19.0		19.2	19.08	1.67		
◺			2.23	37.0	610	306	1.88	[b]7.3	5.97	7.9	5.4	6.4		6.55	6.6	1.88		
◺			2.23	37.0	610	306	1.88	[b]19.9	18.16	20.1	17.6	19.5		21.8	19.75	1.62		
◺			2.46	39.8	610	276	2.06	[b]7.2	6.10	8.1	8.4	6.6		6.6	7.43	1.72		
◺			2.46	39.8	610	276	2.06	[b]10.5	11.09	13.1	13.4	10.6		10.9	12.00	1.58		
◺	7	Wilson	1.72	28.4	610	383	1.52	11.15×10^3	9.02×10^6	7.84	9.4			9.6	8.95		2.49×10^{-3}	θ
▽			1.72	28.4	610	383	1.52	17.1	15.78	14.60	16.2			16.3	15.70		2.18	
◺			2.00	35.4	610	339	1.70	6.97	7.43	8.1	5.4			5.5	6.33		2.20	
◺			2.00	35.4	610	339	1.70	15.18	15.26	15.9	13.2			13.3	14.13		2.14	
◺			2.47	42.0	610	275	2.07	7.79	6.89	5.8	6.5			6.6	6.30		2.47	
◺			2.47	42.0	610	275	2.07	16.61	16.89	15.8	16.5			16.6	16.30		2.04	
◇	20	Wade	2.48	14.0	528	237	2.1		6.33×10^6					4.9	4.9×10^6		2.31×10^{-3}	Drag
◇	21	Monaghan and Cooke	2.82	14.0	552	213	2.44	2.54×10^3	2.4×10^6	2.3	2.0		1.6	2.0	1.98×10^6		2.54×10^{-3}	θ

[a] SFB = Skin-friction balance.
[b] Interpolated value.

TABLE I.- Concluded

SUMMARY OF EXPERIMENTAL DATA TAKEN AT ZERO HEAT TRANSFER

1	2	3	4	5	6	7	8	9	10	11	12	13	14	15	16	17	18	19
Symbol	Ref.	Author	M_δ	p_t, psia	T_t, °R	T_δ, °R	$\frac{T_w}{T_\delta}$	R_θ	R_{le-x}	R_x found from - Extrapolated θ	R_x found from - Ref. 2	R_x found from - $C_f(R_\theta)$	R_x found from - Min. shear	R_x found from - Author's estimate	Average R_x	C_f	C_F	Method of measurement (a)
○	22	Brinich and Diaconis	3.05 3.05	30 50	510 510	178 178	2.67 2.67	3.60×10^3 11.25	4.02×10^6 14.5	3.1 13.7	3.2 14.0			3.5 14.0	3.27×10^6 13.9		2.20×10^{-3} 1.62	θ
▱	23	Goddard	3.07	30	560	194	2.68		8.34×10^6					5.22	5.22×10^6		1.69×10^{-3}	Drag
□ □ □ □ ◇	1	Chapman and Kester	1.99 2.49 2.95 3.36 3.60		530 530 530 530 530	296 237 193 163 148	1.72 2.13 2.59 3.06 3.37							15.0 15.0 15.0 15.0 15.0	15.0×10^6 15.0 15.0 15.0 15.0		2.08×10^{-3} 1.84 1.73 1.57 1.52	Drag
△ ▷ ▽	16	Coles	2.57 2.58 3.70 3.70 4.55 4.55	14.5 25.3 19.9 41.4 58.3 56.4	556 568 561 562 562 554	240 245 150 150 109 108	2.18 2.18 3.43 3.43 4.70 4.70	6.6×10^3 10.2 4.1 7.56 5.11 6.59	4.84×10^6 8.32 3.54 7.25 6.89 6.83			7.4 10.0 3.8 8.4 6.7 9.1	4.5 8.0 3.1 6.8 6.3	6.1 10.3 4.0 8.6 8.2	6.00×10^6 9.43 3.63 7.93 6.70 7.87	1.81×10^{-3} 1.66 1.62 1.38 1.285 1.22		SFB
□	24	Korkegi	5.79 5.79	64.4 109.4	685 685	88 88	6.81 6.81	2.48×10^3 4.04	2.27×10^6 3.86			3.06 5.55		Not given	3.06×10^6 5.55	1.32×10^{-3} 1.18		SFB
△ ▷ ▽ ▽ ▽	25	Matting, et al. These four rows measured in helium	2.95 2.95 4.20 4.20 6.70 6.70 9.90 9.90	35 112 55 500 180 580 630 680	590 590 612 612 610 610 614 614	215 215 135 135 60.7 60.7 29.8 29.8	2.52 2.52 4.07 4.07 8.80 8.80 18.25 18.25	8.27×10^3 22.6 5.45 37.8	9.8×10^6 31.5 7.7 69.6 12.8 41.0 24.3 26.2			8.7 29.0 6.8 76.0		9.0 30.5 6.7 68.2 10.0 40.0 14.7 20.0	8.85×10^6 29.8 6.75 72.1 10.0 40.0 14.7 20.0	1.54×10^{-3} 1.29 1.27 .868 .64 .52 .33 .32		SFB

[a] SFB = Skin-friction balance.

TABLE II

SUMMARY OF EXPERIMENTAL DATA TAKEN WITH HEAT TRANSFER

1	2	3	4	5	6	7	8	9	10	11	12	13	14	15	16	17	18	19
										R_x found from -								
Symbol	Ref.	Author	M_δ	p_t, psia	T_t, °R	T_δ, °R	$\frac{T_w}{T_\delta}$	R_θ	R_{le-x}	Extrapolated θ	Ref. 2	$C_f(R_\theta)$	Min. shear	Author's estimate	Average R_x	C_f	C_F	Method of measurement
◇	26	Pappas	1.69	26	578	378	1.65	4.34×10^3	2.68×10^6	1.3	2.6			2.8	2.23×10^6		3.89×10^{-3}	θ
◇			1.69	42	578	378	1.61	9.78	7.65	5.5	7.2			7.7	6.80		2.88	
◇			2.27	30	578	284	2.18	2.93	2.44	2.2	1.7			1.9	1.93		3.04	
◇			2.27	45	578	284	2.12	9.40	7.87	10.2	7.5			7.8	8.50		2.21	
▷	27	Monaghan and Cooke	2.43	13.8	426	196	3.43	5.57×10^3	4.39×10^6	3.9	4.2		4.0	4.4	4.13×10^6		2.70×10^{-3}	θ
▷			2.43	13.8	497	229	2.94	3.51	2.70	4.7	2.5		2.4	2.5	3.03		2.32	
○	21	Monaghan and Cooke	2.82	13.8	497	192	3.50	3.39×10^3	3.04×10^6	2.2	2.8		2.6	2.9	2.63×10^6		2.58×10^{-3}	θ
□	28	Swanson, Buglia, and Chauvin	2.89	84	992	371	2.15		62×10^6					47	47×10^6		1.36×10^6	θ
□			3.31	231	1,275	400	1.86		94					79	79		1.43	
□			3.53	385	1,421	407	1.71		115					100	100		1.33	
△	11	Winkler and Cha	5.14	103	849	135	3.67	3.26×10^3	4.22×10^6	3.1	2.9			Not given	3.00×10^6		2.175×10^{-3}	θ
▽			5.22	101	693	107	4.89	3.79	5.11	3.1	3.9				3.50		2.165	
▽			5.25	105	664	102	5.51	4.30	5.94	3.7	5.6				4.65		1.85	
⌂	3	Sommer and Short	2.81	403	1,385	536	1.03		3.16×10^6					0.63 to 3.00	1.65	2.84×10^{-3}		Drag
⌂			3.78	1,685	2,110	546	1.05		4.26					1.75 to 4.94	2.75	2.04		
⌂			3.82	1,745	2,123	542	1.05		4.26					0.88 to 4.07	2.27	2.27		
⌂			5.63	7,140	3,290	448	1.29		4.58					1.05 to 4.71	3.16	1.70		
⌂			6.90	15,500	3,470	330	1.71		4.16					2.00 to 5.07	3.39	1.25		
⌂			7.00	24,400	3,560	330	1.75		6.28					3.28 to 8.00	5.13	1.15		
▽	29	Hill	8.27		1,360	93	6.19	2.51×10^3				2.8		3.7	3.25×10^6	0.840×10^{-3}		Velocity slope
▽			9.07		1,360	78	8.30	2.28				3.6		3.8	3.70	.870		
▽			10.04		1,480	70	9.38	1.45				1.8		2.5	2.15	.761		

TABLE III

SUMMARY OF THEORIES

Theory	$C_F{}^*$	$R_x{}^*$
Van Driest (Prandtl mixing length)	$\frac{C_{F,w}}{\phi^2}$	$\frac{R_{x,w}\phi^2}{(T_w/T_\delta)^{1/2}}$
Wilson and Van Driest (Von Kármán mixing length)	$\frac{C_{F,w}}{\phi^2}$	$R_{x,w}\phi^2$
Cope and Monaghan	$C_{F,w}$	$\frac{R_{x,w}}{T_w/T_\delta}$
Winkler and Cha	$C_F \frac{(T_t/T_\delta)^{1/2}}{(T_w/T_{aw})^{1/4}}$	$R_x \frac{(T_w/T_{aw})^{1/4}}{(T_t/T_\delta)^{1/2}}$
Sommer and Short T', Monaghan T', and Eckert T'	$C_{F,T'}$	$R_{x,T'}$

$$C_{F,w} = \frac{D/S}{\frac{1}{2}\rho_w U_\delta{}^2} \qquad C_{F,T'} = \frac{D/S}{\frac{1}{2}\rho' U_\delta{}^2}$$

$$R_{x,w} = \frac{\rho_w U_\delta x}{\mu_w} \qquad R_{x,T'} = \frac{\rho' U_\delta x}{\mu'}$$

$$\phi = \frac{1}{A}\left[\sin^{-1}\frac{A - \frac{B}{2A}}{\sqrt{1 + \left(\frac{B}{2A}\right)^2}} + \sin^{-1}\frac{\frac{B}{2A}}{\sqrt{1 + \left(\frac{B}{2A}\right)^2}}\right]$$

$$A^2 = \frac{T_{aw}}{T_w} - \frac{T_\delta}{T_w} \qquad B = \frac{T_{aw}}{T_w} - 1$$

Sommer and Short:

$$\frac{T'}{T_\delta} = 1 + 0.035M^2 + 0.45\left(\frac{T_w}{T_\delta} - 1\right)$$

Monaghan:

$$\frac{T'}{T_\delta} = 1 + 0.0284M^2 + 0.54\left(\frac{T_w}{T_\delta} - 1\right)$$

Eckert:

$$\frac{T'}{T_\delta} = 1 + 0.0392M^2 + 0.5\left(\frac{T_w}{T_\delta} - 1\right)$$

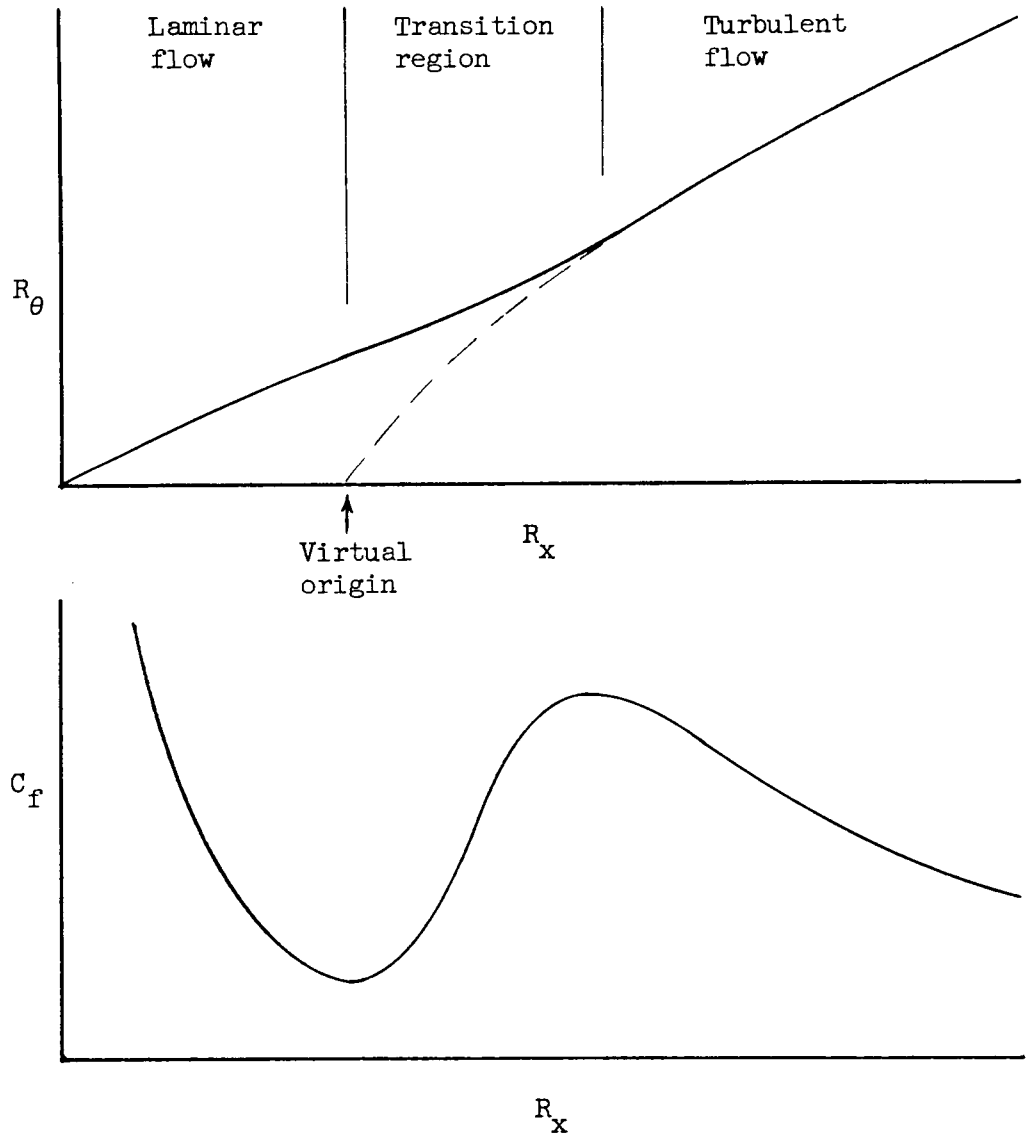

Figure 1.- Boundary-layer growth and shear distribution on a flat plate.

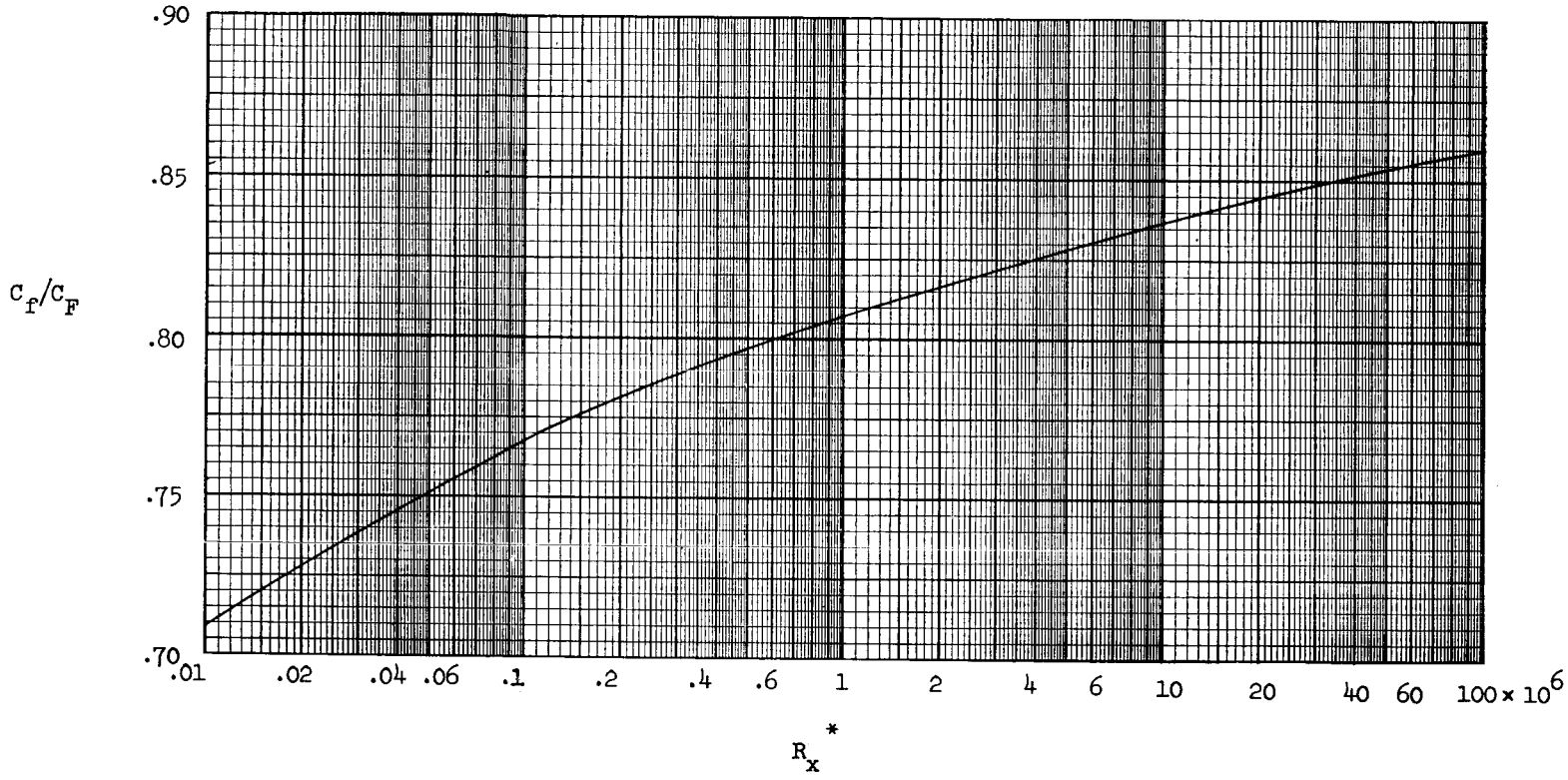

Figure 2.- Ratio of local to average turbulent skin-friction coefficient from the Kármán-Schoenherr formula.

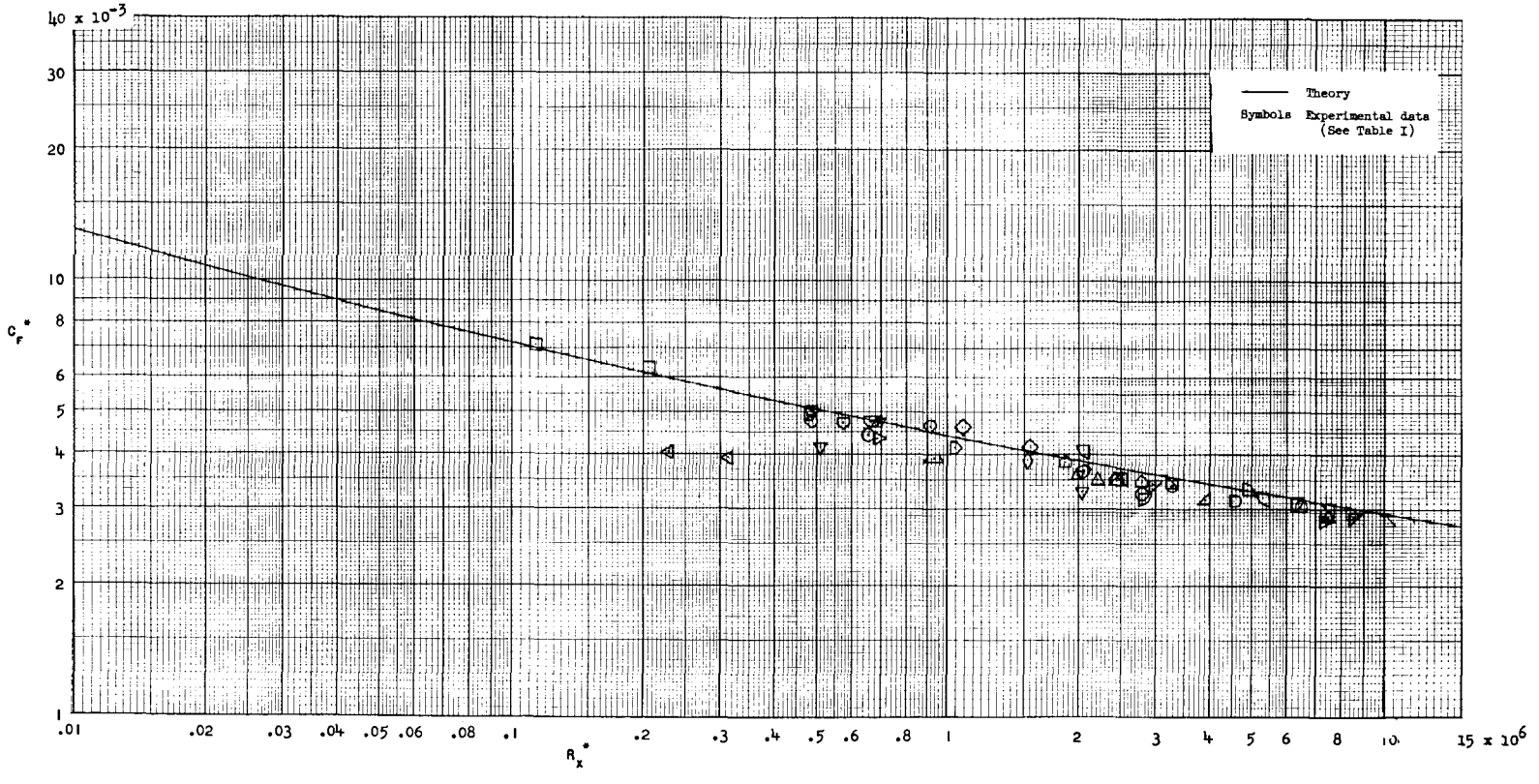

Figure 3.- Compressible turbulent skin-friction data at zero heat transfer reduced by Wilson's and Van Driest's theories. (Von Kármán mixing length.)

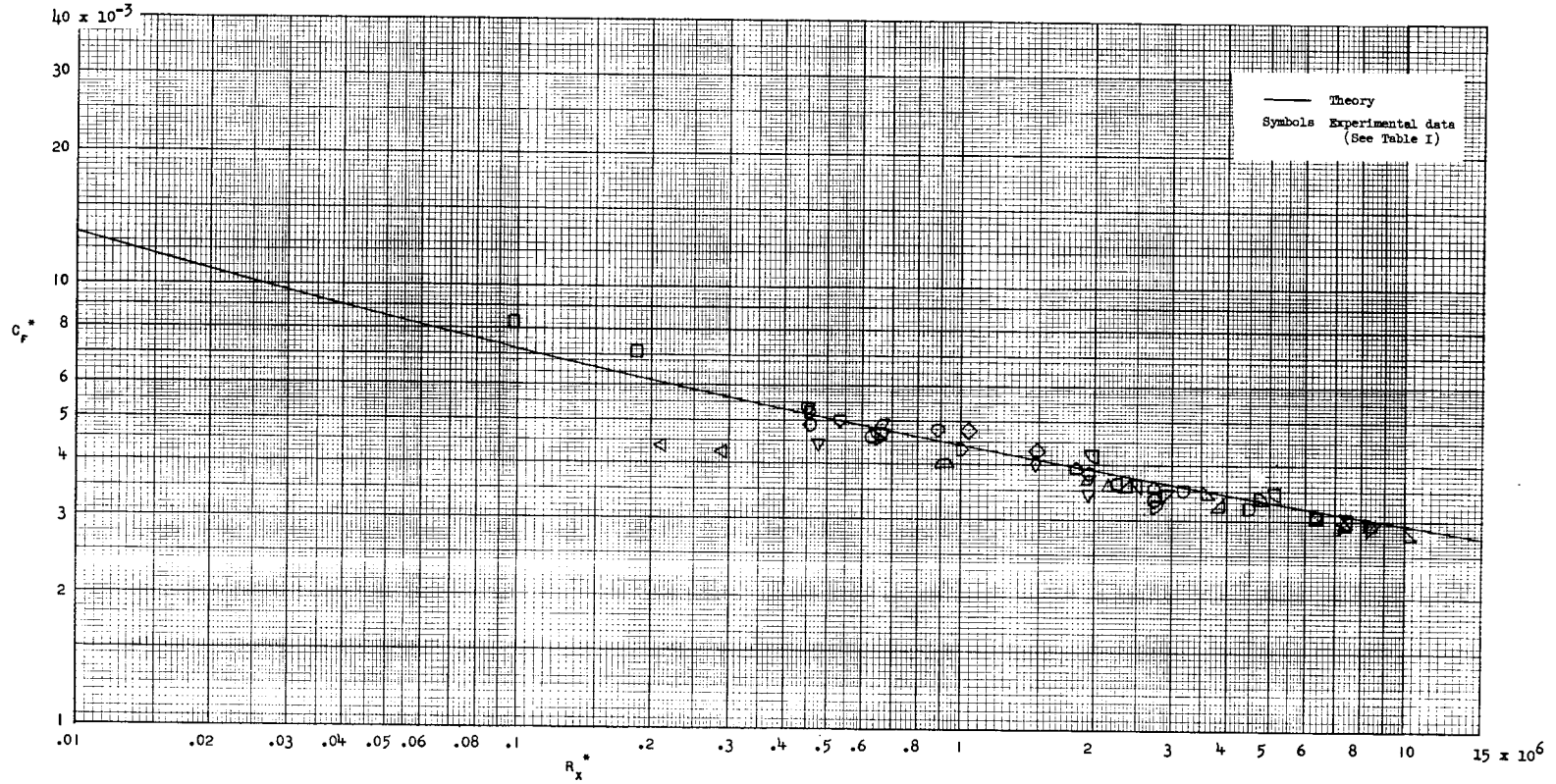

Figure 4.- Compressible turbulent skin-friction data at zero heat transfer reduced by Wilson's and Van Driest's theories with sublayer included. (Von Kármán mixing length.)

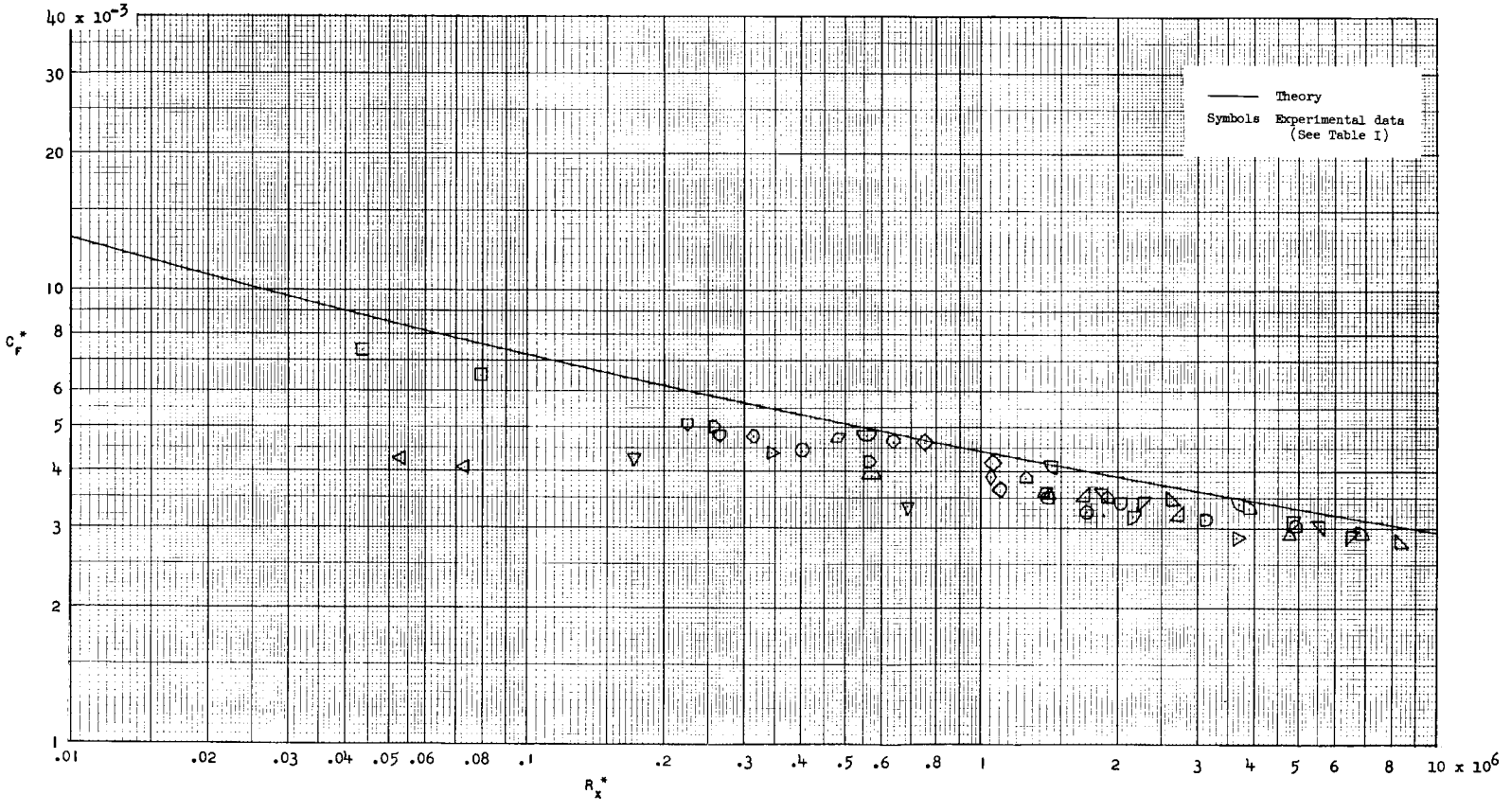

Figure 5.- Compressible turbulent skin-friction data at zero heat transfer reduced by Van Driest's theory. (Prandtl mixing length.)

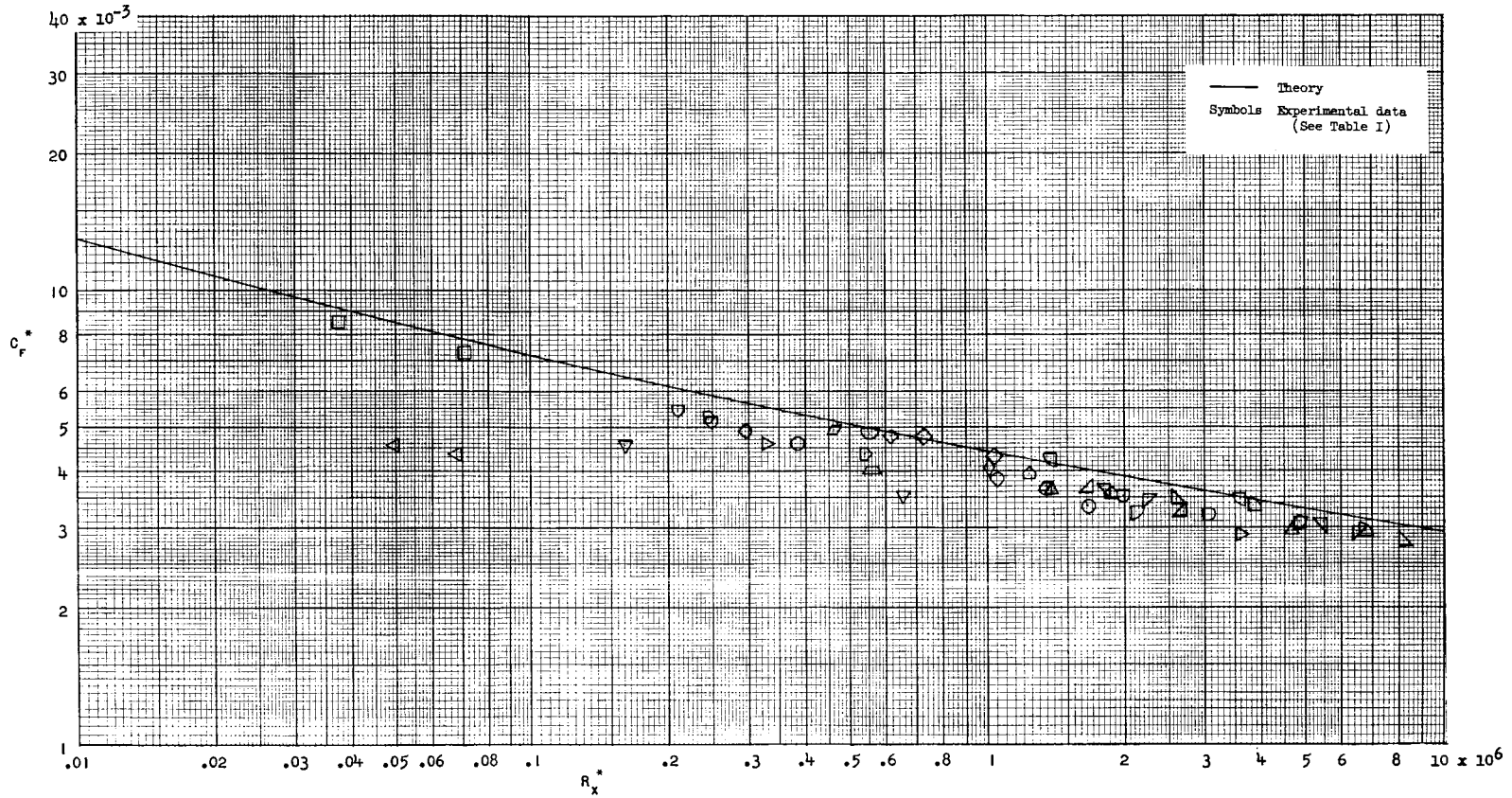

Figure 6.- Compressible turbulent skin-friction data at zero heat transfer reduced by Van Driest's theory with sublayer included. (Prandtl mixing length.)

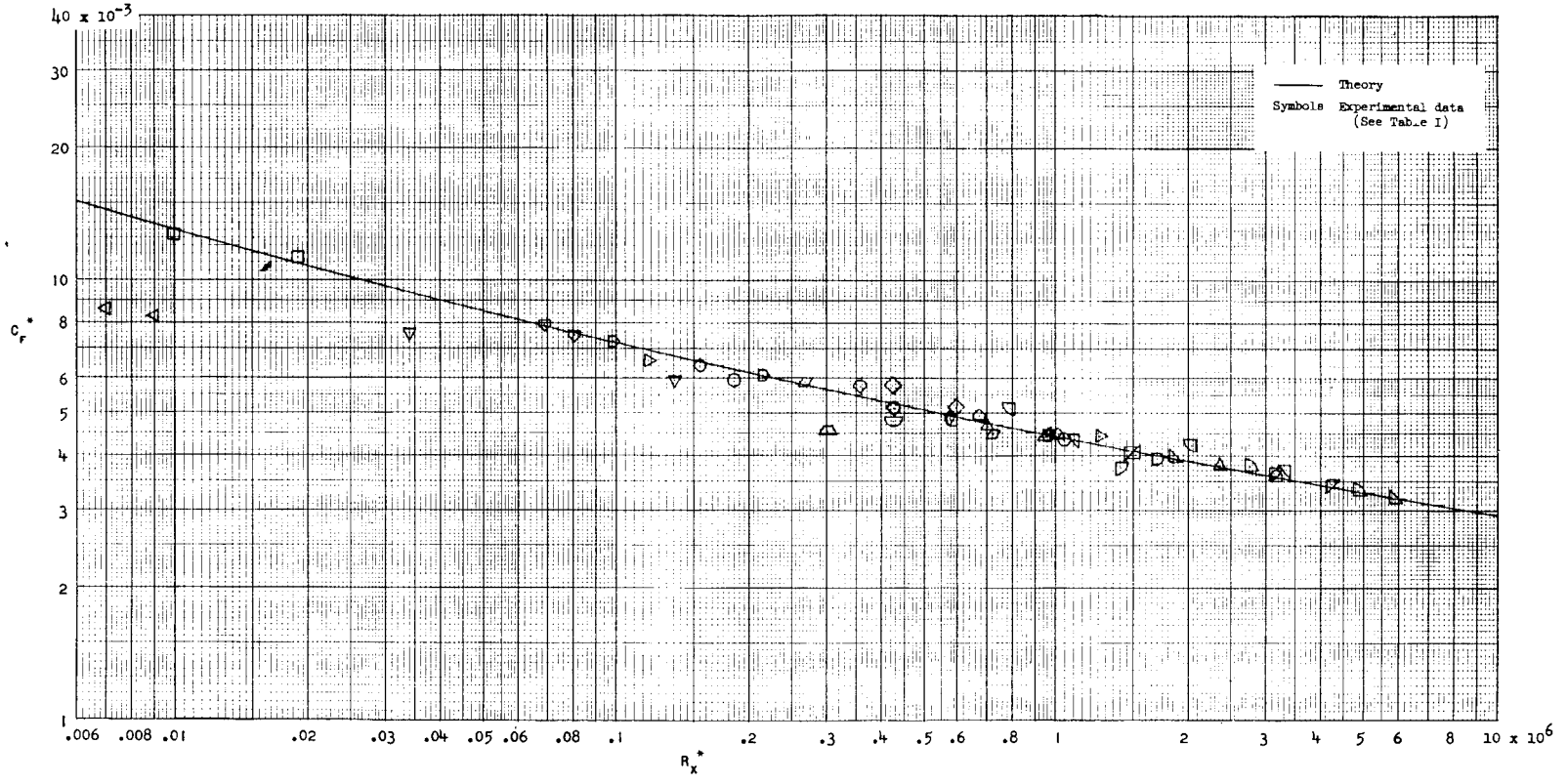

Figure 7.- Compressible turbulent skin-friction data at zero heat transfer reduced by Cope's and Monaghan's theories.

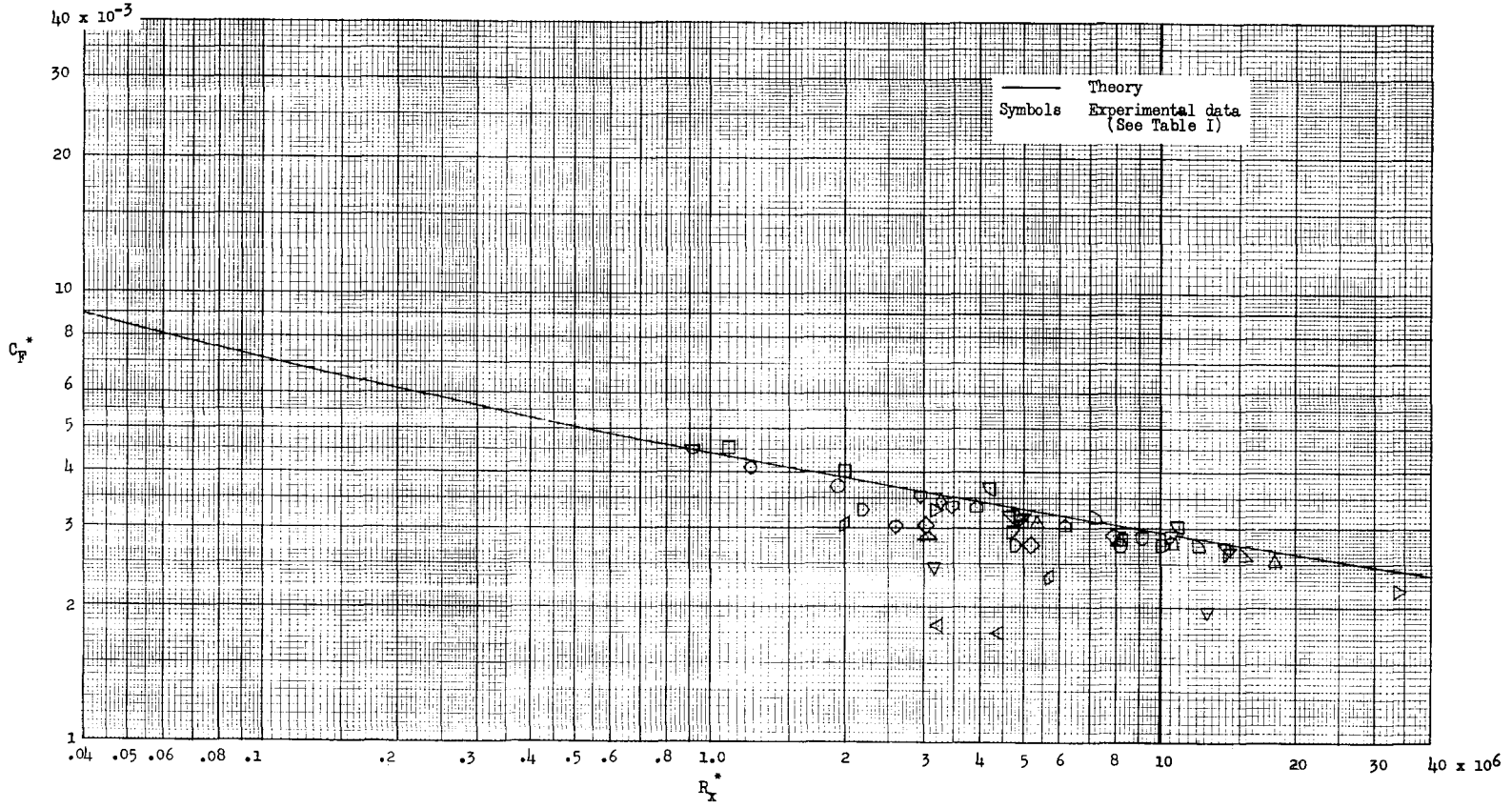

Figure 8.- Compressible turbulent skin-friction data at zero heat transfer reduced by Winkler and Cha's method.

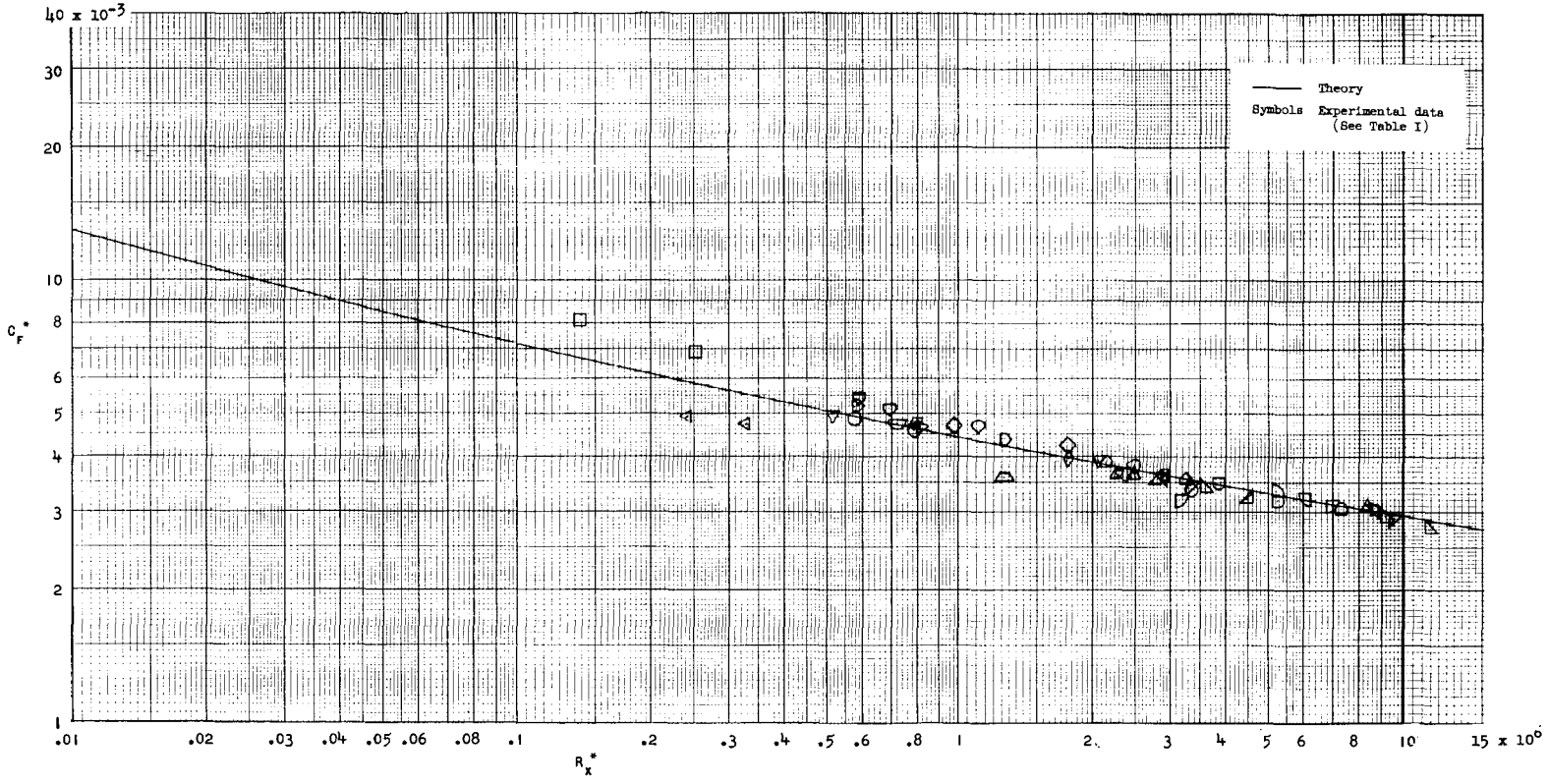

Figure 9.- Compressible turbulent skin-friction data at zero heat transfer reduced by Sommer and Short's T' method.

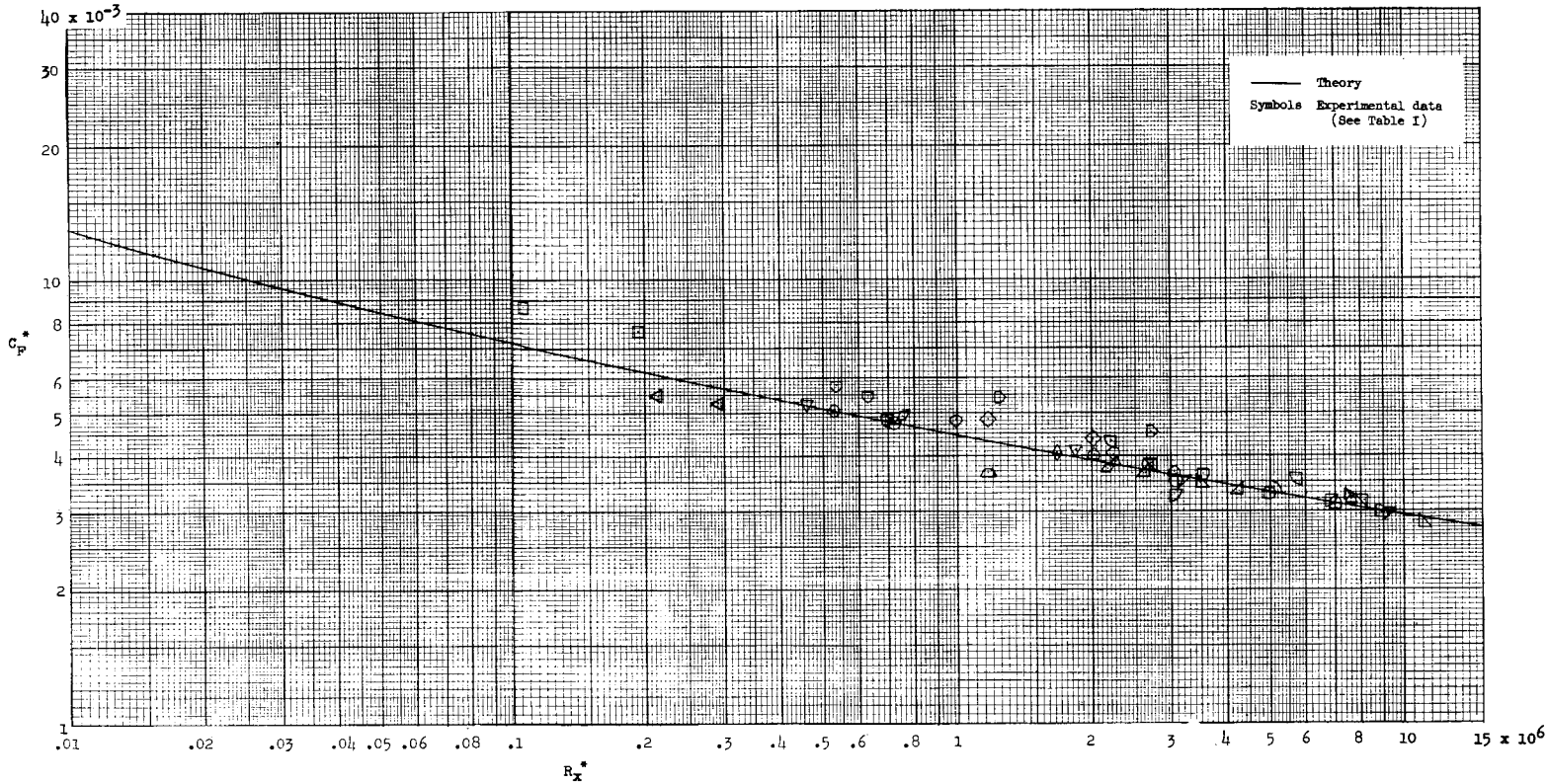

Figure 10.- Compressible turbulent skin-friction data at zero heat transfer reduced by Monaghan's T' method.

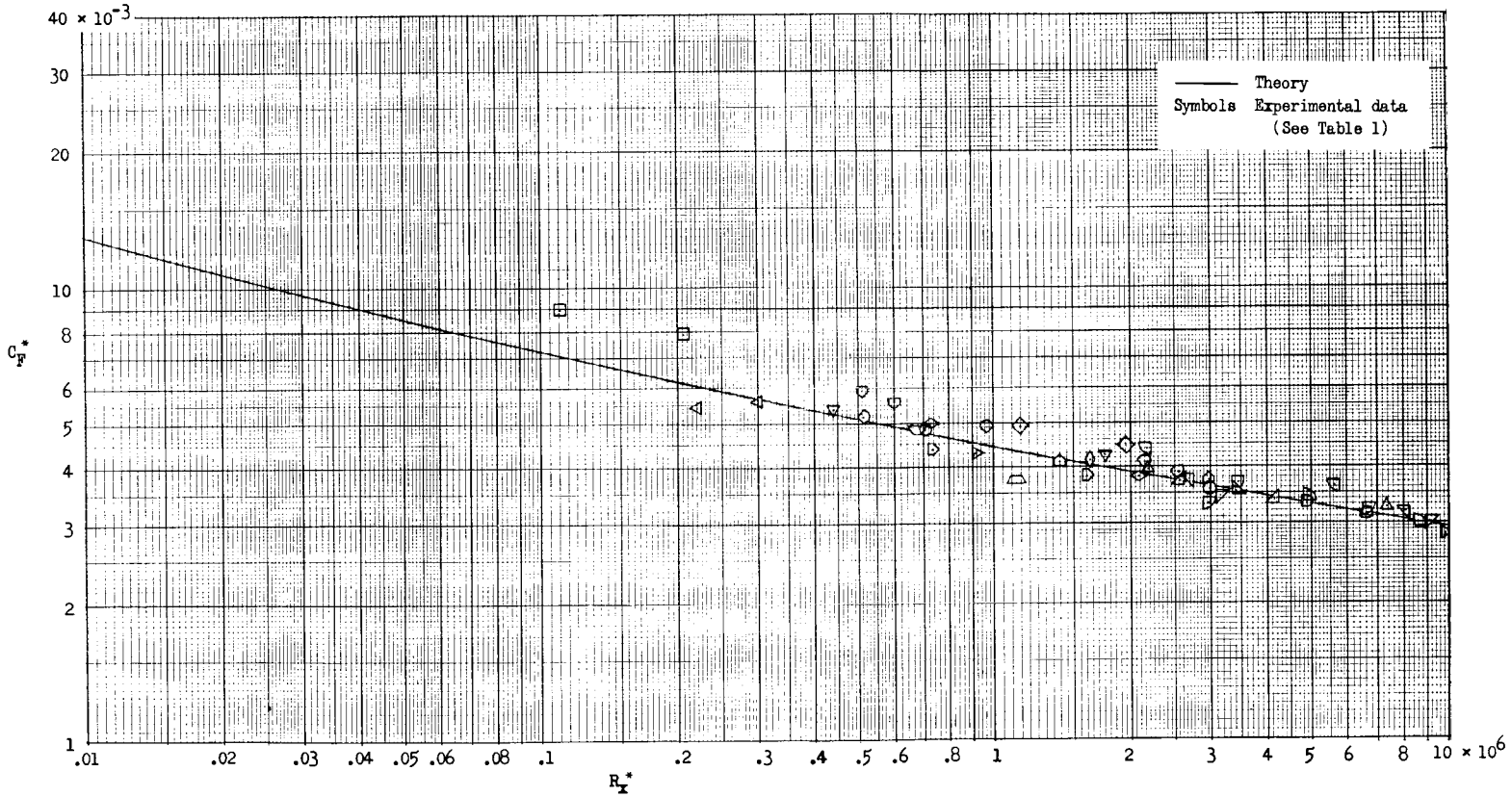

Figure 11.- Compressible turbulent skin-friction data at zero heat transfer reduced by Eckert's T' method.

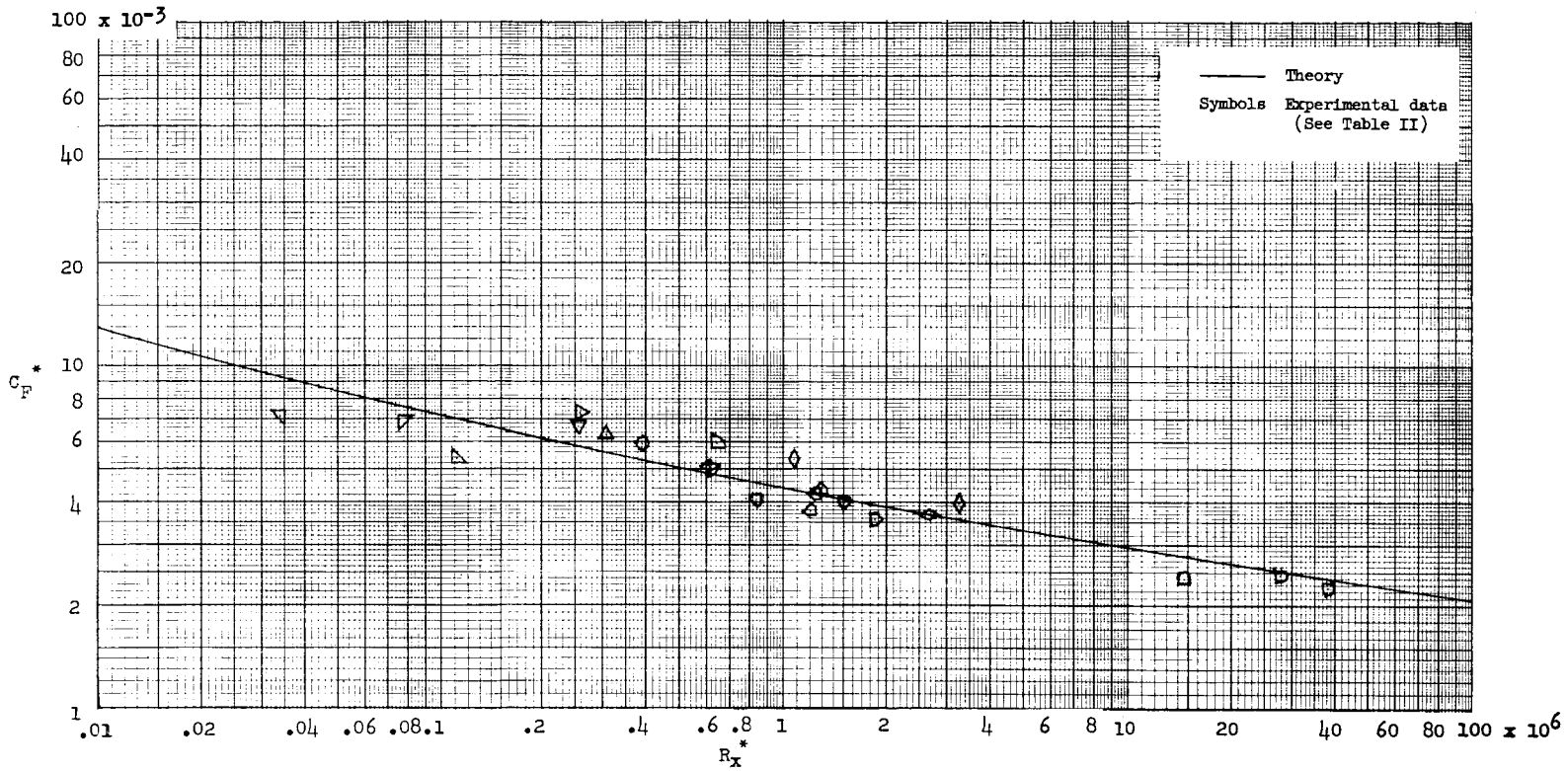

Figure 12.- Compressible turbulent skin-friction data with heat transfer reduced by Wilson's and Van Driest's theories. (Von Kármán mixing length.)

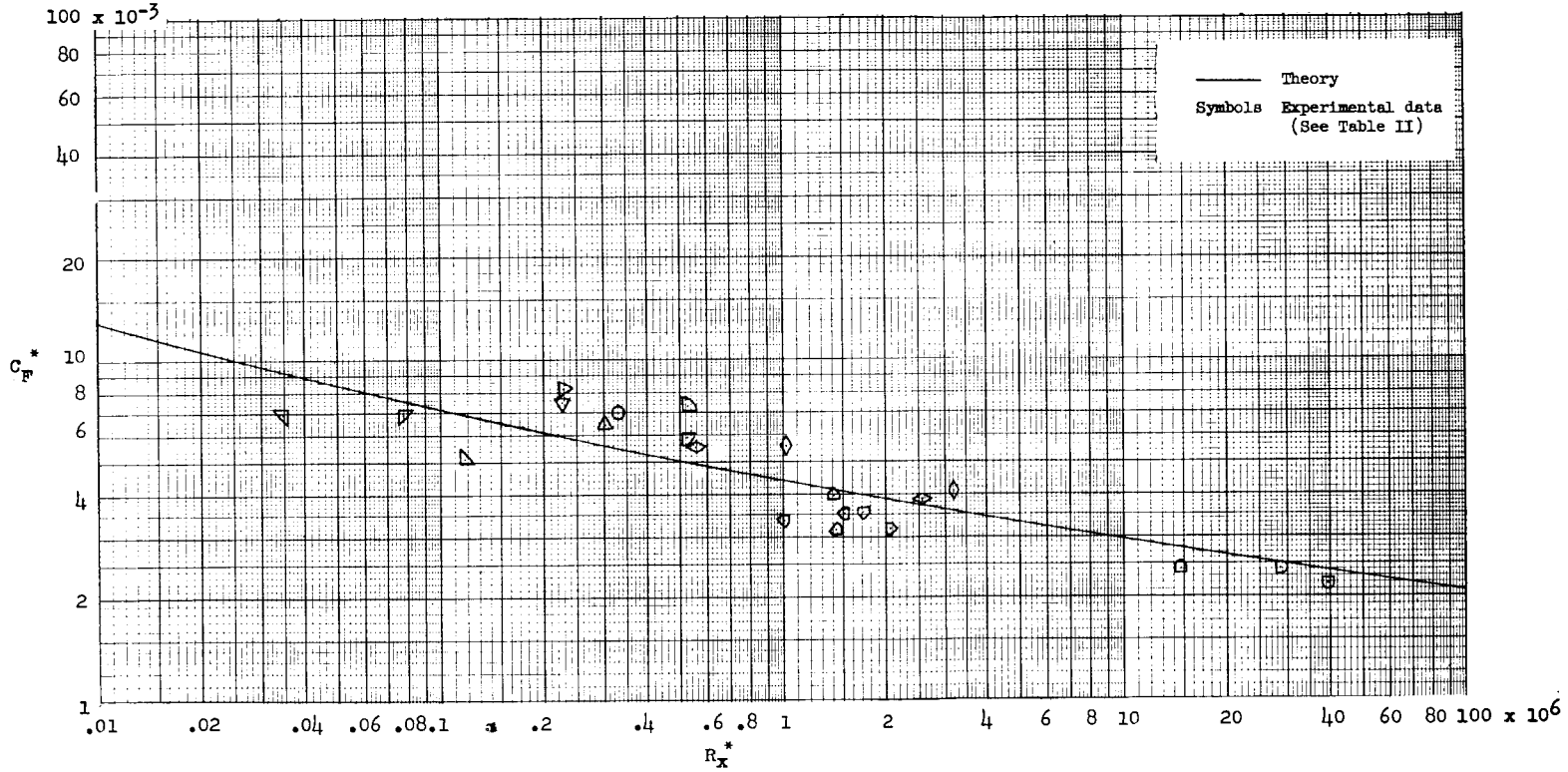

Figure 13.- Compressible turbulent skin-friction data with heat transfer reduced by Wilson's and Van Driest's theories with sublayer included. (Von Kármán mixing length.)

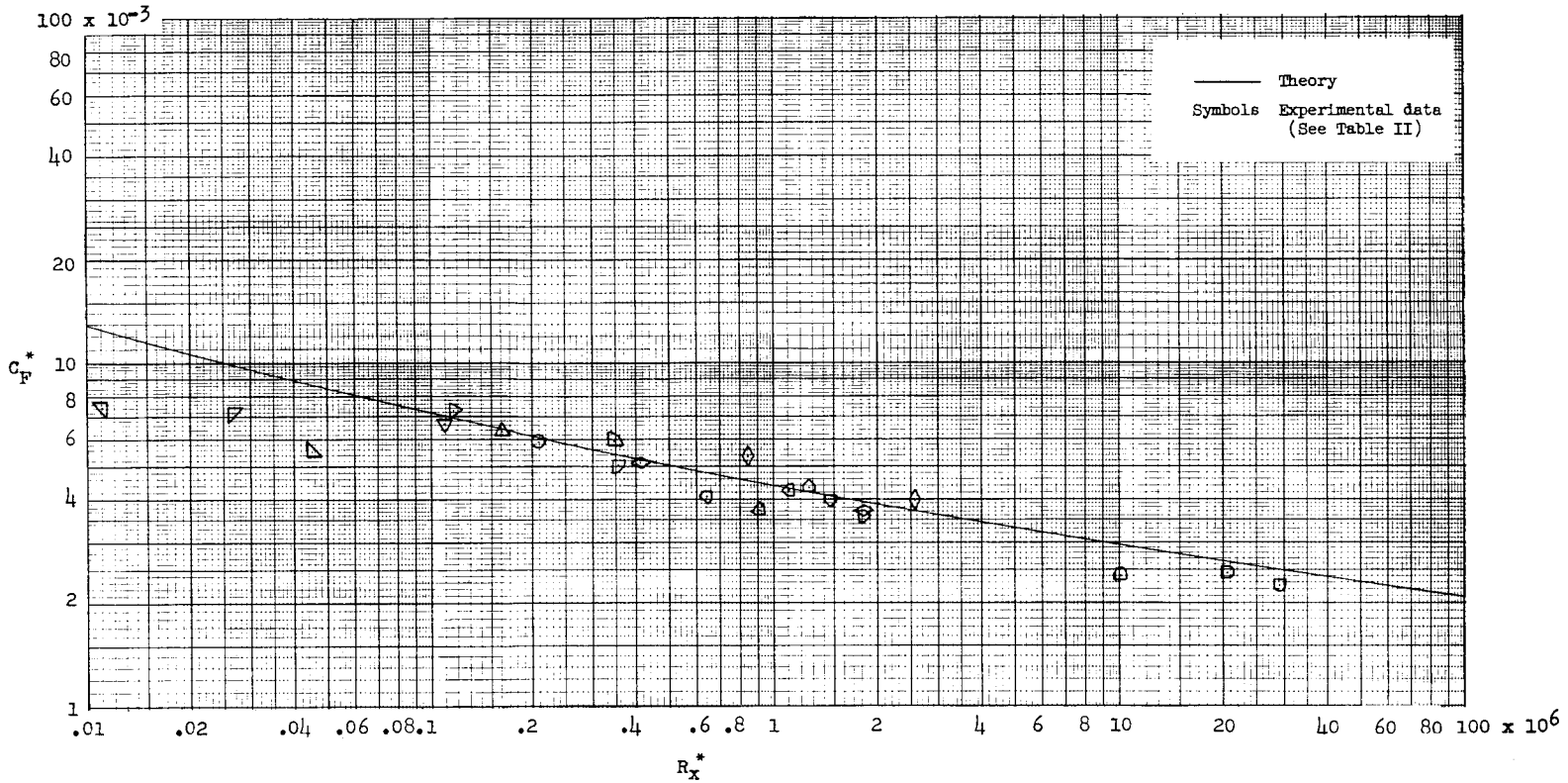

Figure 14.- Compressible turbulent skin-friction data with heat transfer reduced by Van Driest's theory. (Prandtl mixing length.)

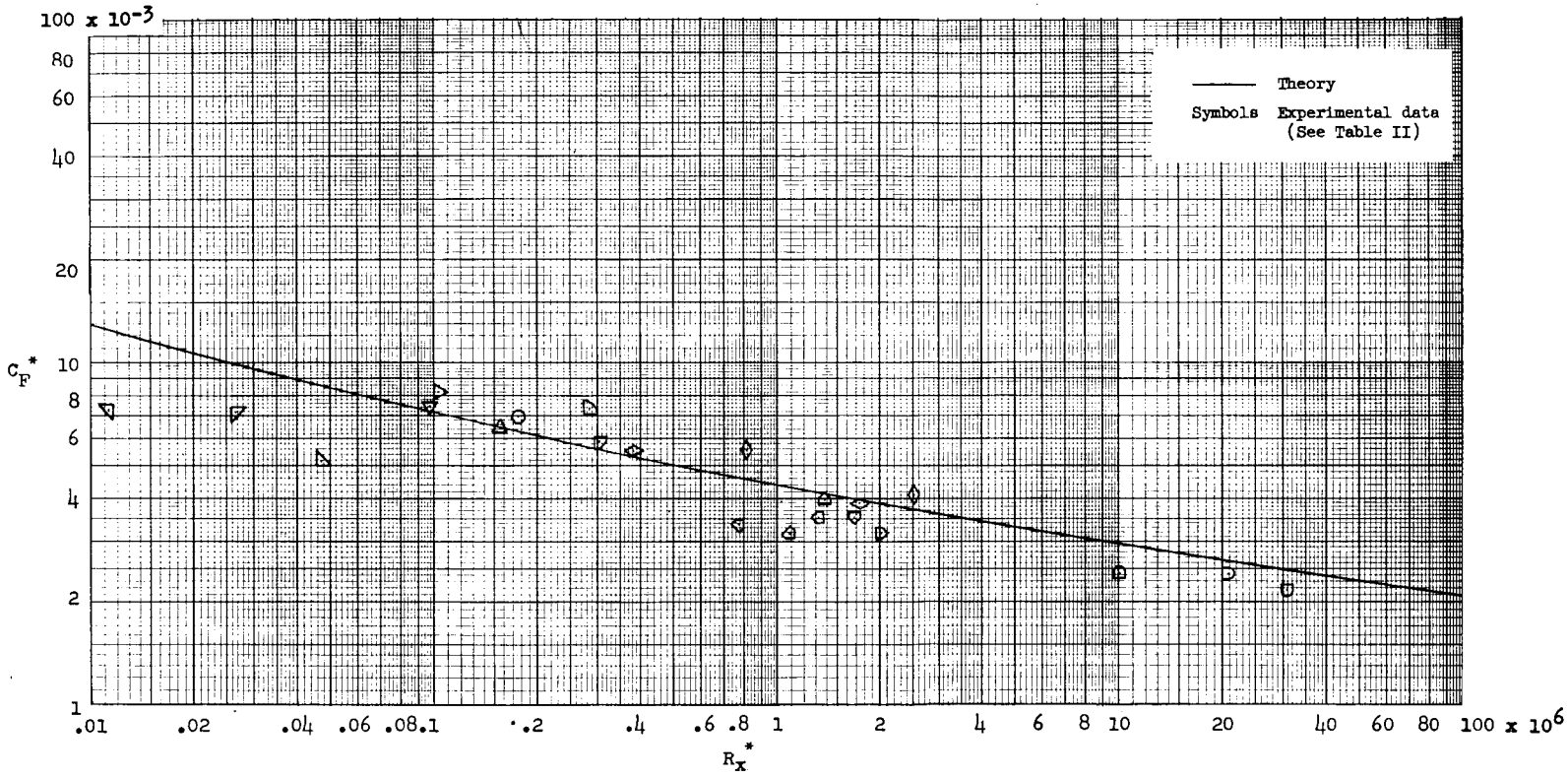

Figure 15.- Compressible turbulent skin-friction data with heat transfer reduced by Van Driest's theory with sublayer included. (Prandtl mixing length.)

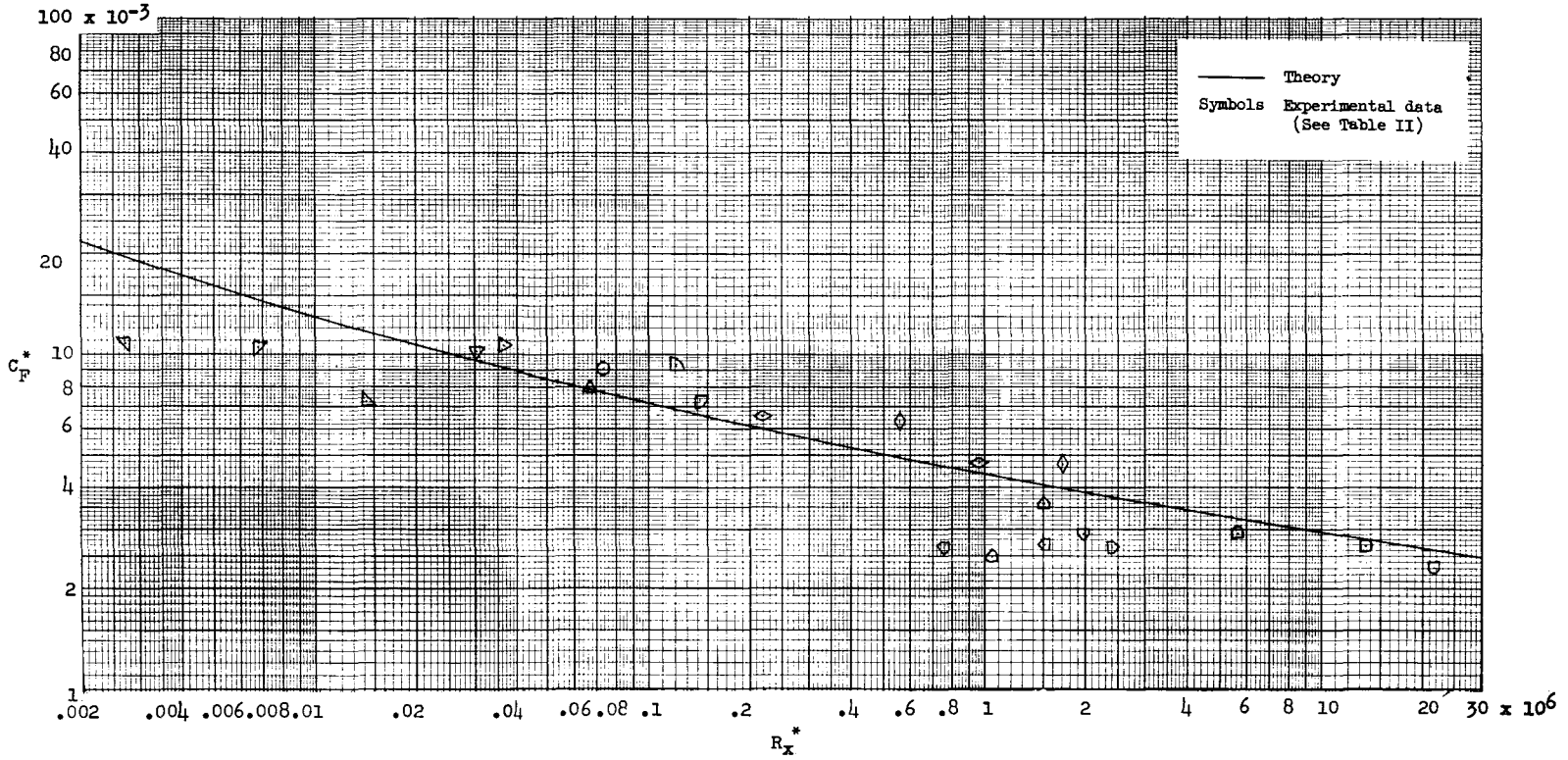

Figure 16.- Compressible turbulent skin-friction data with heat transfer reduced by Cope's and Monaghan's theories.

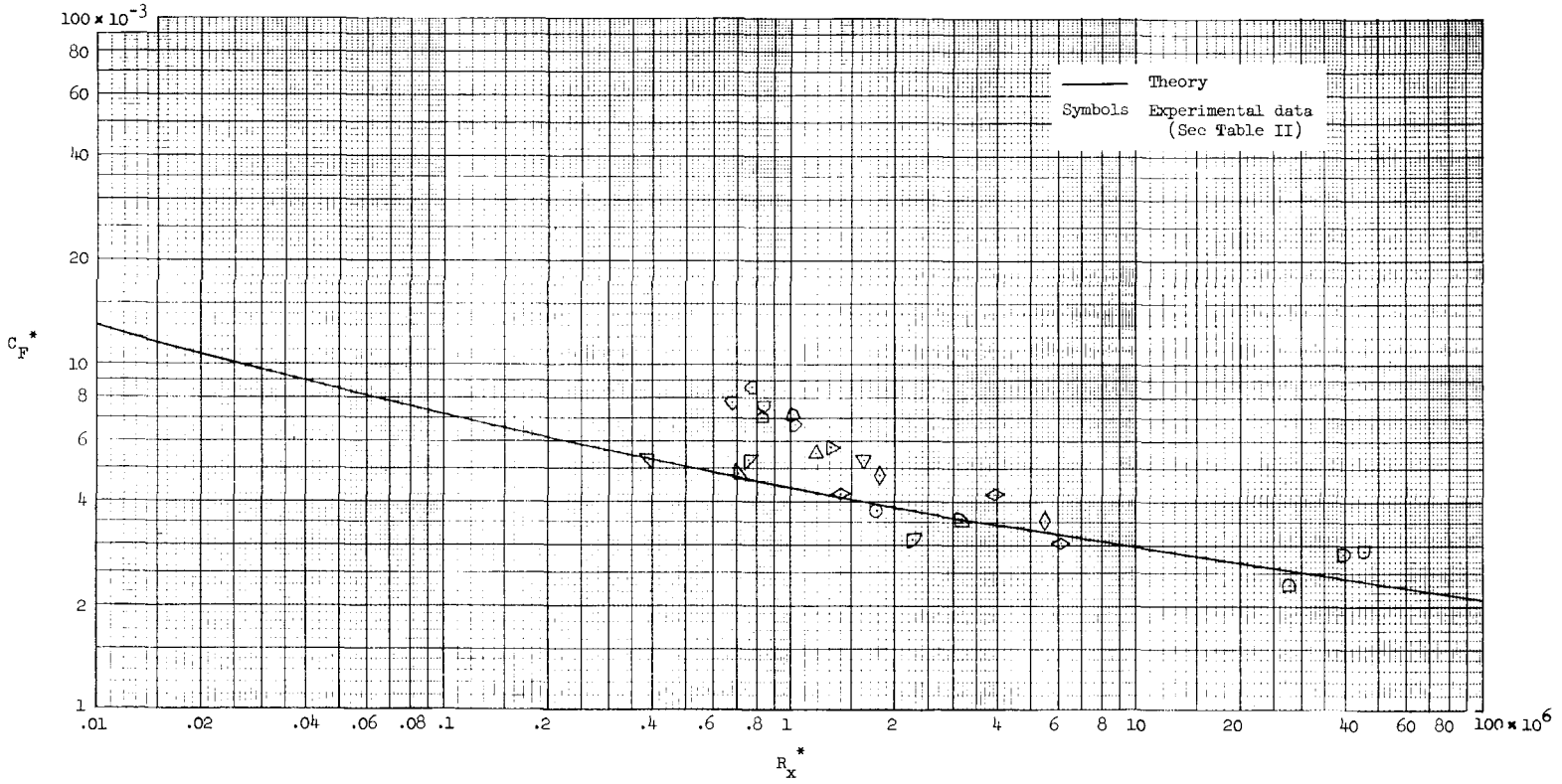

Figure 17.- Compressible turbulent skin-friction data with heat transfer reduced by Winkler and Cha's theory.

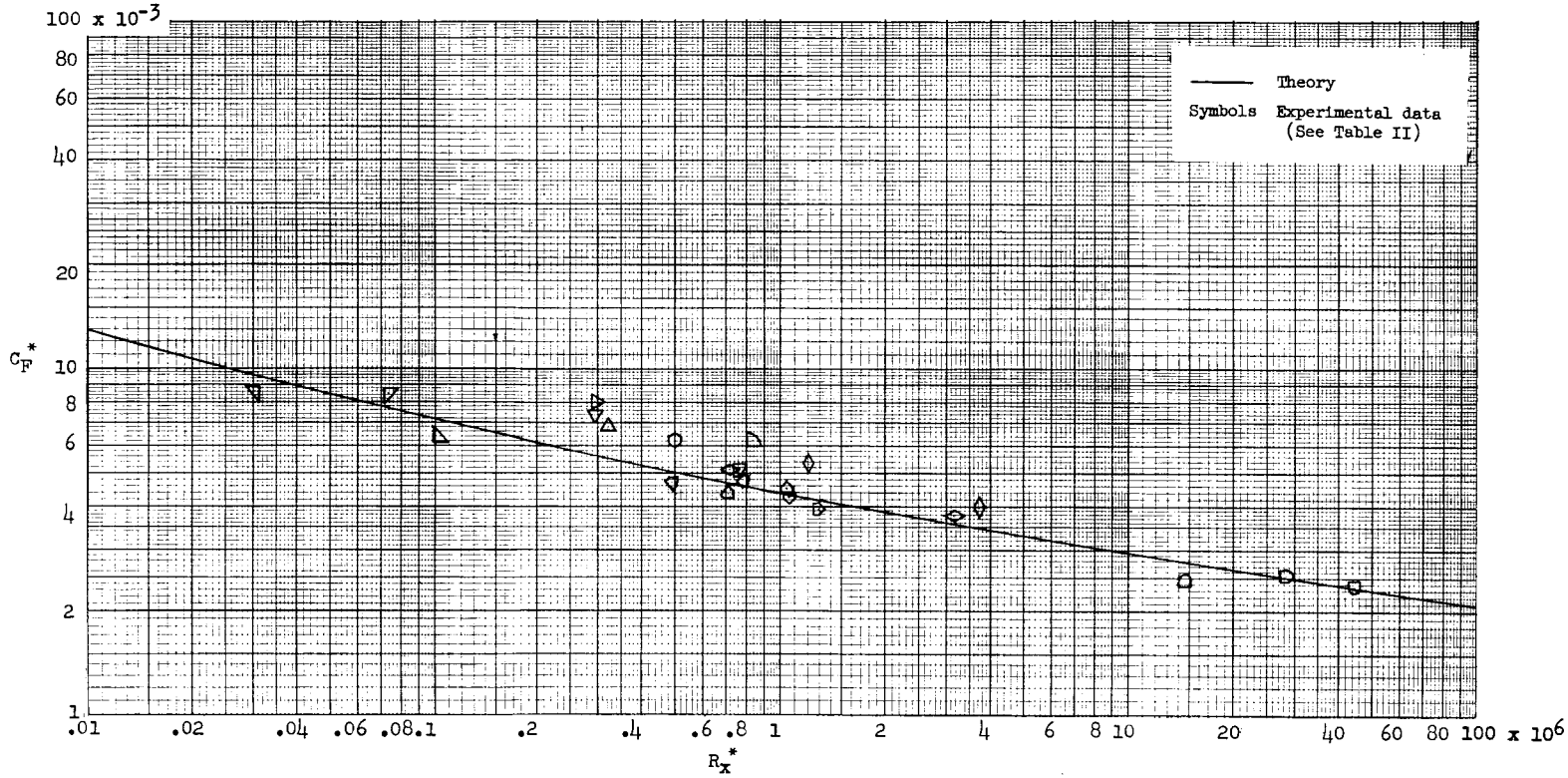

Figure 18.- Compressible turbulent skin-friction data with heat transfer reduced by Sommer and Short's T' method.

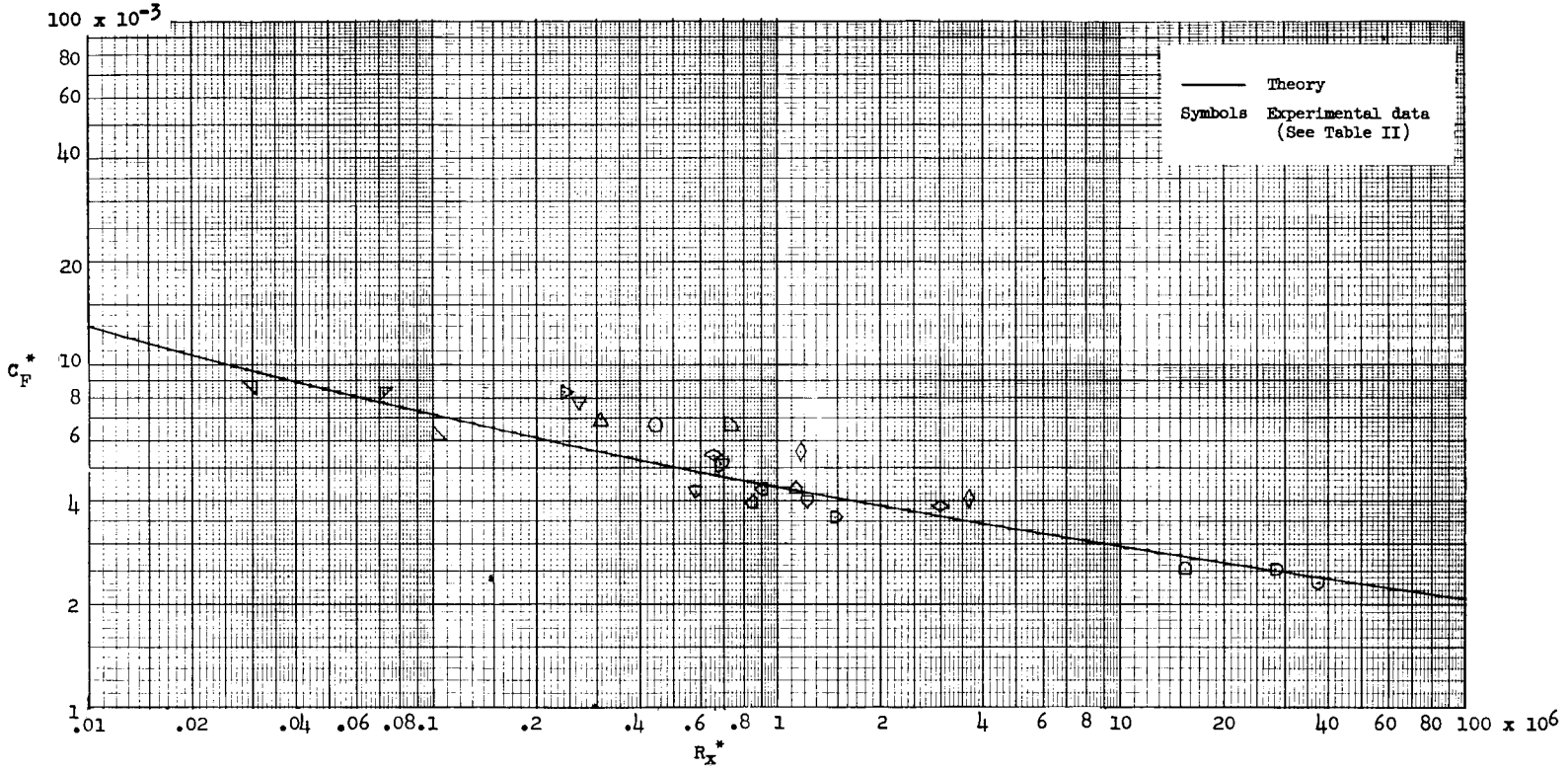

Figure 19.- Compressible turbulent skin-friction data with heat transfer reduced by Monaghan's T' method.

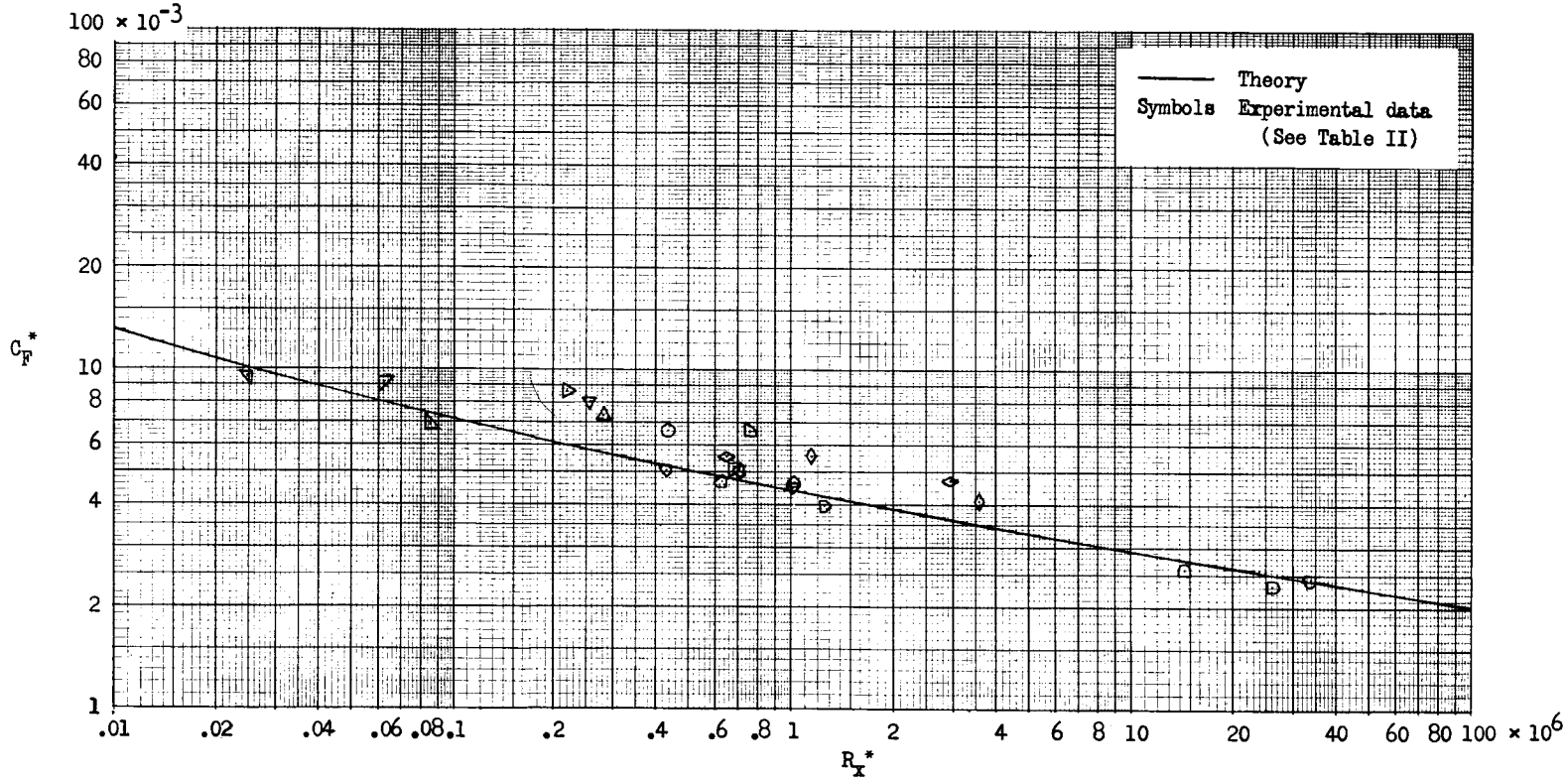

Figure 20.- Compressible turbulent skin-friction data with heat transfer reduced by Eckert's T' method.

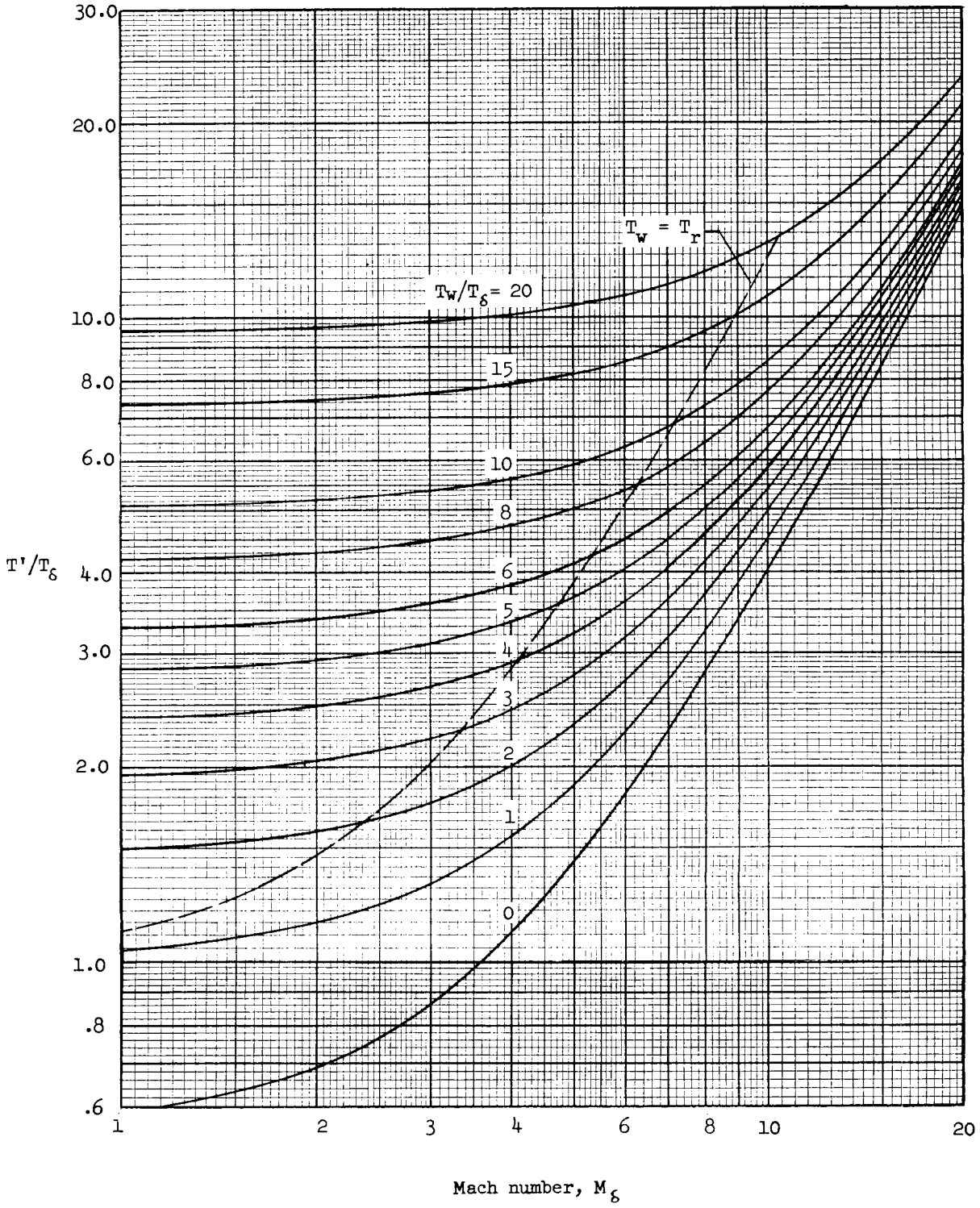

Figure 21.- Reference-temperature ratio by the Sommer and Short T' method.

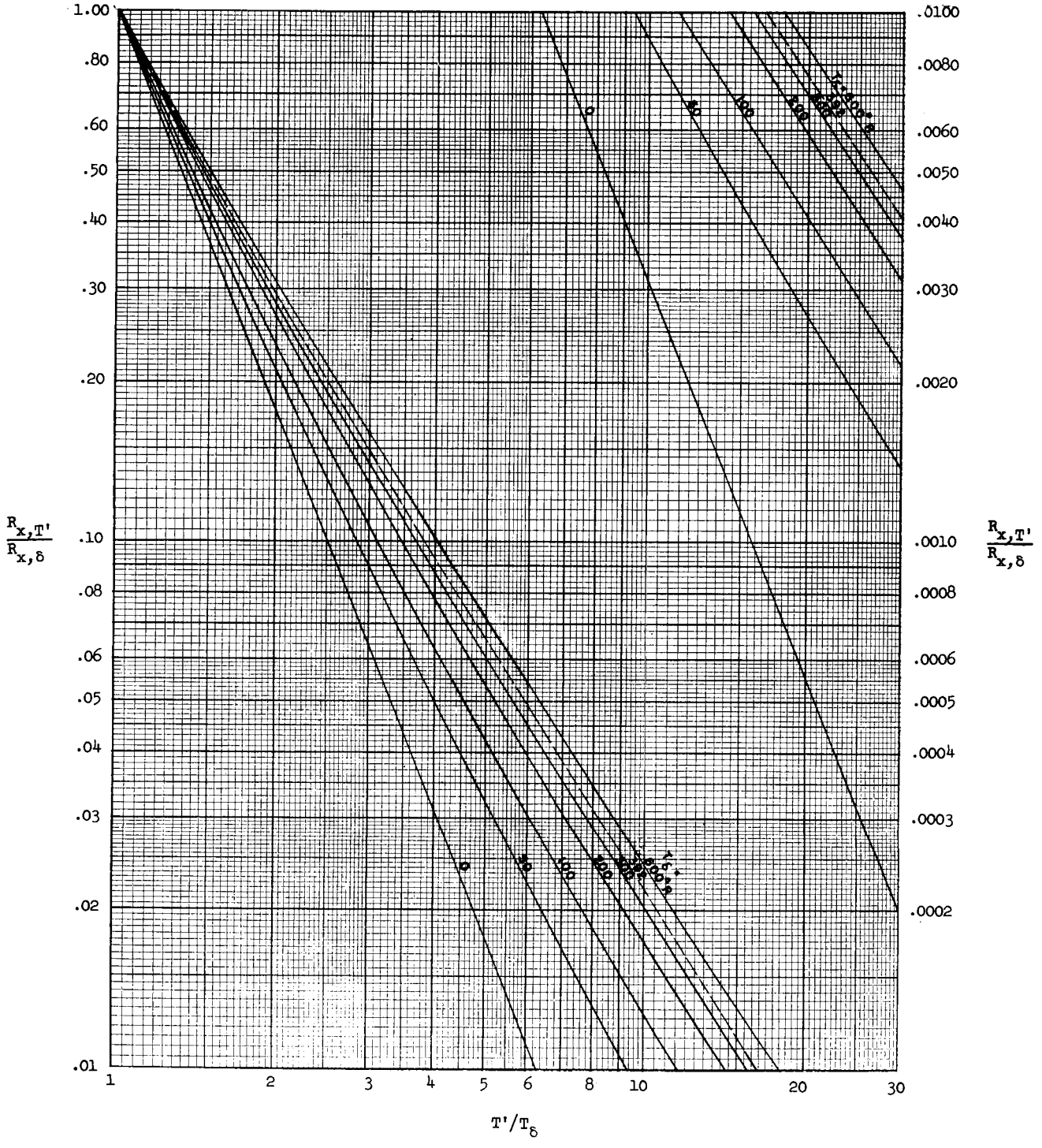

Figure 22.- Reynolds number ratio.

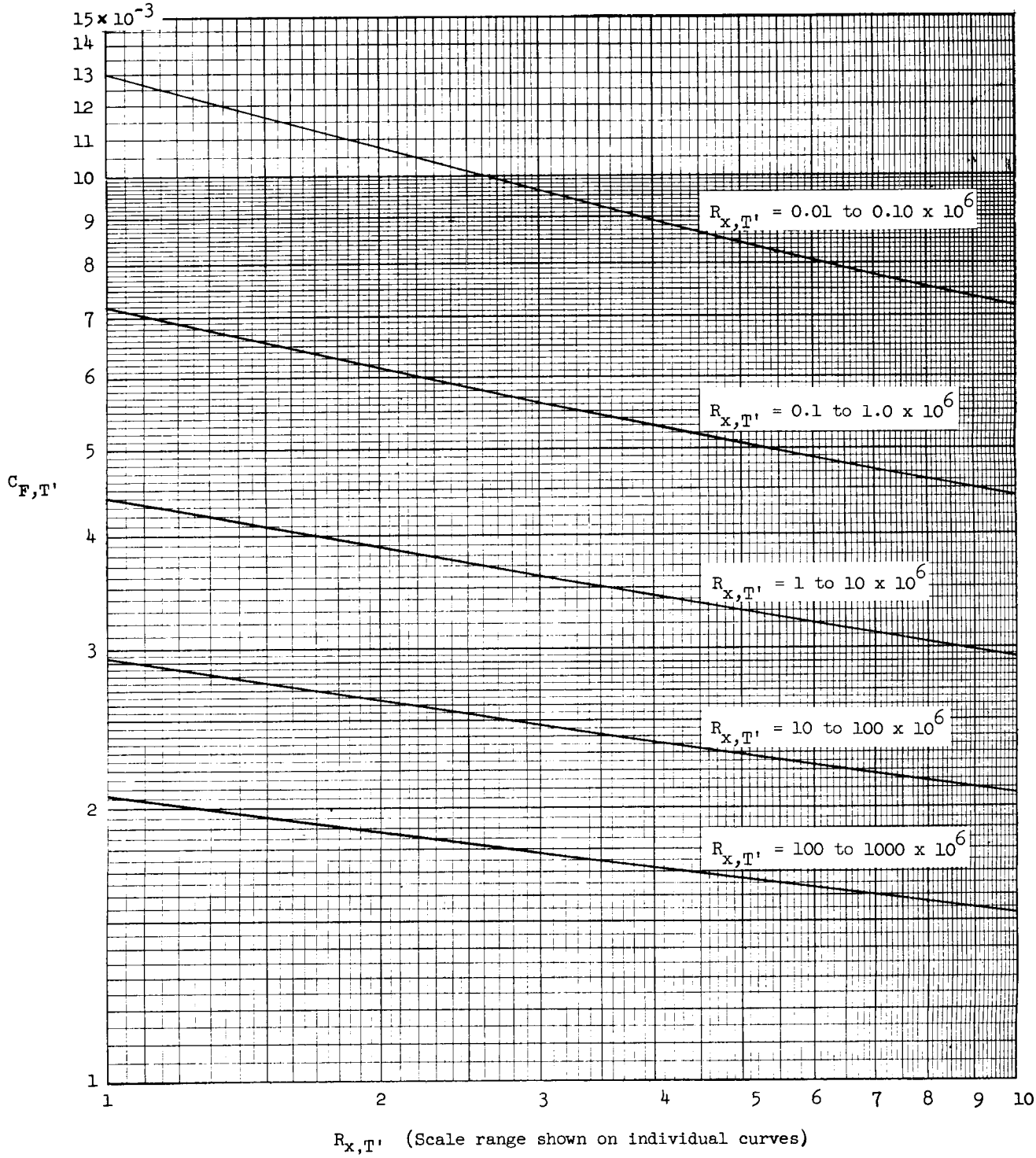

Figure 23.- Average turbulent skin-friction coefficient based on T' from Kármán-Schoenherr formula.

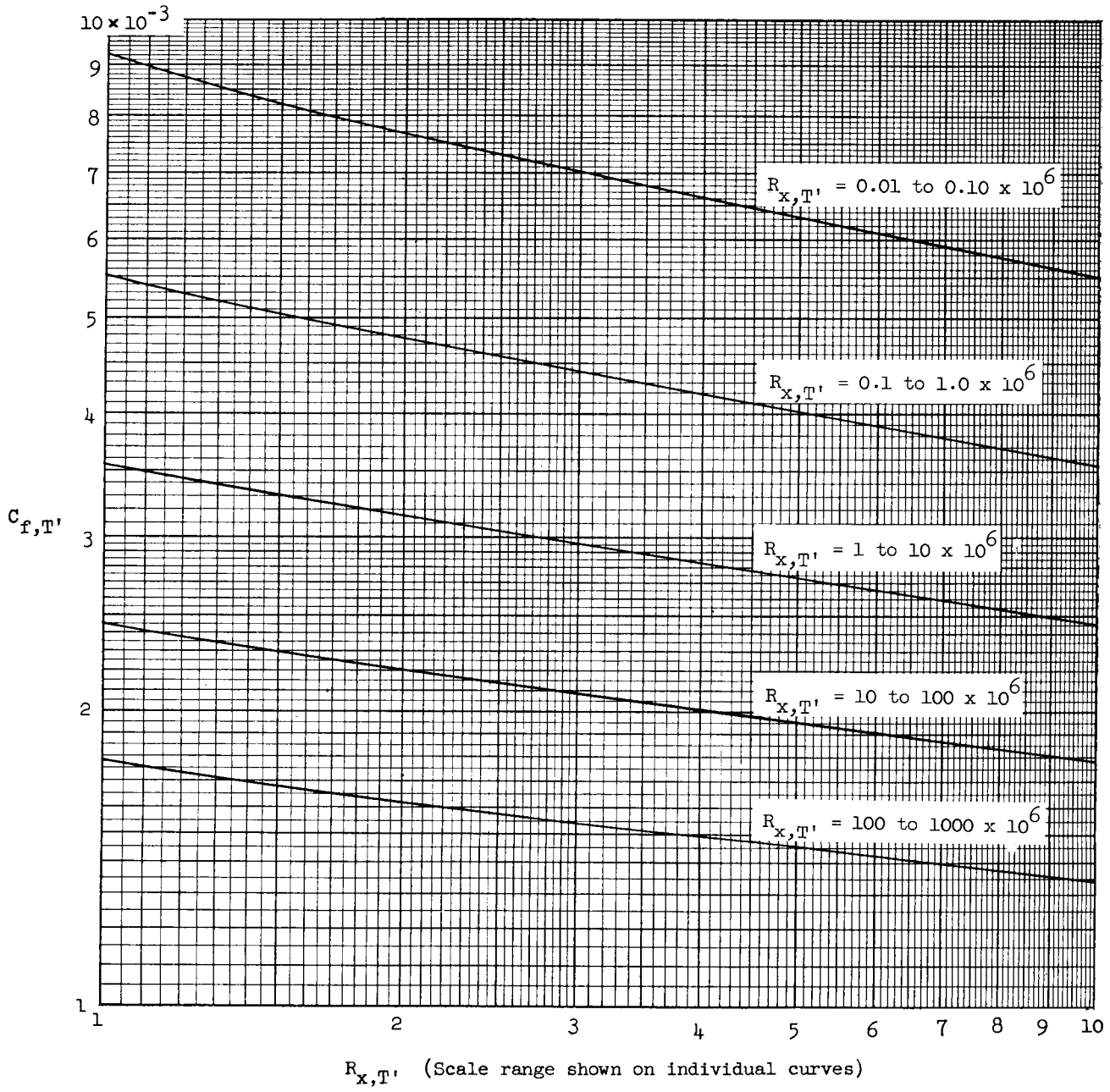

Figure 24.- Local turbulent skin-friction coefficient based on T' from Kármán-Schoenherr formula.